

Lecture II

Diffraction of light



principles of geometrical optics indicate that the propagation of light is influenced by the presence of obstacles in its path in a manner determined by the form and properties of the obstacles. A polished metallic sphere, for instance, would reflect the light falling upon it and hence would cast a shadow. More complicated would be the effects due to a transparent obstacle, e.g., a drop of water, as both the reflections and refractions at its surface would have to be considered. The determination of the resulting light intensity everywhere in

the field in a case of this kind is a problem in the theory of diffraction. It is evident that the indications of geometrical optics must be supplemented by those of the wave-theory, in view of the possibility of interference arising between rays of light which cross each other after traversing different paths. In the case of the metallic sphere, for instance, the entire field outside the region of shadow should exhibit interferences between the incident and reflected rays. Similarly in the case of the liquid drop, the interferences between the direct and refracted rays would, in addition, need to be considered. The question also arises whether the conclusions derived from ray optics remain valid in all circumstances. In the particular case of the metallic sphere, for instance, the geometric shadow is sensibly perfect in the vicinity of the sphere, but at a sufficient distance behind it, observation reveals the presence of a bright spot of light at the centre of the shadow. How is this fact to be reconciled with the concepts of ray optics?

It is evident that the study of diffraction raises a fundamental issue, namely, the relationship between the ray and wave concepts of light. An adequate discussion of diffraction phenomena necessarily includes a consideration of these two aspects of optical theory and a reconciliation between them. The geometric approach provided by ray optics has the merit of simplicity and enables us to obtain an intuitive grasp of the phenomena. Hence, instead of considering

diffraction phenomena as falling solely within the scope of wave-optics and as indicative of a failure of geometrical optics, it is a much more satisfactory procedure to bring diffraction within the scope of ray optics by appropriately framing our fundamental concepts. How this may be done is illustrated by the optical effects produced by a corrugated surface which we shall now consider in some detail.

Refraction of light by a corrugated surface: The phenomena which we shall now consider may be experimentally studied with a ripple tank, utilizing the fact that the surface of a liquid agitated by a linear system of ripples of definite frequency and wavelength is a corrugated surface. A narrow slit illuminated by a mercury lamp and followed by a collimating lens may be used as the source of light. The beam after passing through the liquid surface or after reflection by it is viewed through a telescope focussed for parallel rays. We may consider here a parallel beam of light which passes vertically upwards through a ripple tank containing

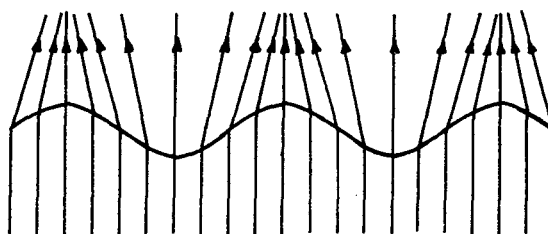


Figure 32. Rays emerging from ripple tank.

water. Figure 32 represents the geometric courses of the rays of light on emergence from the liquid. The rays would be divergent over the concave areas and convergent over the convex areas of the surface, but at a sufficiently great distance would be divergent throughout. These elementary considerations of ray optics describe correctly the effects observed in the immediate vicinity of the surface. But at points sufficiently removed from the surface, they no longer represent the facts correctly.

We may ask ourselves, why is the geometric theory valid near the surface of the liquid and why does it apparently fail at points sufficiently far removed from it? The answer to these questions must be found in the fact that the disturbance on emergence from the liquid surface is no longer a simple train of plane waves. As remarked earlier in our discussion on the interference of light, *the principle of*

rectilinear propagation of light and the principle of interference do not in any way contradict each other. But if apparent contradictions are to be avoided, it is necessary that we should recognise only waves of constant type on the one hand, and the rays normal to them on the other, as the proper basis for the description of the optical field. In our present problem, for instance, we should analyse the disturbance on emergence from the liquid surface into its component plane waves. The subsequent movement of such plane waves along their respective normals would furnish a description of the optical effects which is equally correct from the wave and the ray points of view and which is valid for every part of the field, both near and far from the surface of the liquid.

We have already seen (figure 2) that two plane wave-trains superposed on each other result in a stratification of the amplitude and phase of the disturbance in the field. The spacing $2D$ of such stratifications measured in a plane bisecting the angle between the wave-fronts is given by the formula $2D \sin \psi = \lambda$. This relation may be readily generalised. The superposition of sets of wave-trains travelling in various directions lying in a common plane and making angles ψ_n with some fixed direction in it, the relation $2D \sin \psi_n = n\lambda$ being satisfied, ($n = 0, \pm 1, \pm 2$, etc.), would result in the most general type of disturbance in which the amplitude and phase vary periodically in the plane normal to the fixed direction. Hence, putting $2D = \lambda^*$, where λ^* is the wavelength of the ripples, we may represent the light emerging from the liquid surface by such a set of plane waves travelling along the directions ψ_n given by the formula $\lambda^* \sin \psi_n = n\lambda$, ($n = 0, \pm 1, \pm 2$, etc.). Accordingly, when the light is viewed through a telescope focussed for infinity, a set of monochromatic images of the original light source would be observed on either side of the original direction of the light beam. The directions and intensities of these images would correspond to the plane waves into which the disturbance emerging from the liquid surface has been analysed. It will be noticed that the formula is the well known one for the diffraction spectra due to a grating, but it has been obtained here directly from fundamental concepts, without introducing the principle of Huyghens.

Figure 2 gives us other useful indications regarding the geometric character of the optical effects to be expected in our problem. Consider the pair of wave-trains proceeding along the directions $\psi_{\pm n}$. As shown by the figure, the space periods of the resultant disturbance perpendicular to the fixed direction and parallel to it are respectively $\lambda/\sin \psi_n$ and $\lambda/\cos \psi_n$. Hence, the resultants of the wave-trains $\psi_0, \psi_{\pm 1}, \psi_{\pm 2}, \psi_{\pm 3}$, etc., have space periods $\infty, \lambda^*, \lambda^*/2, \lambda^*/3$, etc., along any plane normal to the fixed direction, thus being in strict harmonic relationship. Along the fixed direction, however, the "wavelengths" of the resultants are $\lambda, \lambda/\cos \psi_1, \lambda/\cos \psi_2, \lambda/\cos \psi_3$, etc. As these lengths are not identical the resultant disturbance would fluctuate as we proceed away from the liquid surface along the light beam. It can be readily shown that the disturbance would undergo a periodic cycle of changes, repeating itself completely when we advance a distance $2\lambda^{*2}/\lambda$ or any

multiple of it, away from the surface. This is verified on putting $p\lambda = (p - n^2)\lambda/\cos\psi_n$, where p is an integer, and using the approximation

$$\cos\psi_n = (1 - \psi_n^2/2) = (1 - n^2\lambda^2/2\lambda^{*2}).$$

We obtain immediately $p\lambda = 2\lambda^{*2}/\lambda$. In other words, the result of superposing the waves $\psi_{\pm 1}$ on ψ_0 would repeat itself *once* when we advance a distance $2\lambda^{*2}/\lambda$, while that of superposing $\psi_{\pm n}$ on ψ_0 would repeat itself n^2 times within the same range. The appearance of the light field would, therefore, show fluctuations of a complex periodic character as we move away from the liquid surface, the spacing of the whole cycle being $2\lambda^{*2}/\lambda$.

An expression is readily found for the amplitudes of the plane wave-trains into which the disturbance emerging from the liquid surface is analysed. The light vector in the emergent wave when the surface of the liquid is plane may be taken proportional to

$$\sin(2\pi vt - 2\pi z/\lambda) = \sin Q.$$

The retardation of phase produced at a given epoch by ripples of amplitude 'a' progressing along the y -axis is

$$2\pi a(\mu - 1)/\lambda \cdot \cos 2\pi y/\lambda^*.$$

We shall denote this for brevity by $v \cdot \cos \phi$. Accordingly, the expression for the light vector as modified by the presence of the ripples is proportional to $\sin(Q - v \cos \phi)$. This may be expanded and written in the form

$$\begin{aligned} J_0(v) \sin Q - J_1(v) [\cos(Q + \phi) + \cos(Q - \phi)] \\ - J_2(v) [\sin(Q + 2\phi) + \sin(Q - 2\phi)] \\ + J_3(v) [\cos(Q + 3\phi) + \cos(Q - 3\phi)] \\ + J_4(v) [\sin(Q + 4\phi) + \sin(Q - 4\phi)], \text{ etc.} \end{aligned}$$

It is easily verified that the terms $\sin Q$, $\cos(Q \pm \phi)$, $\sin(Q \pm 2\phi)$, etc., represent plane waves travelling along the directions we have already indicated as $\psi_0, \psi_{\pm 1}, \psi_{\pm 2}$, etc. The intensities of these waves are accordingly proportional to $J_0^2(v)$, $J_1^2(v)$, $J_2^2(v)$, etc. As extensive tables of the Bessel functions are available, these quantities may be readily found for any assigned value of v . It may be remarked that, as is to be expected,

$$J_0^2(v) + 2J_1^2(v) + 2J_2^2(v) + 2J_3^2(v) + \dots = 1,$$

so that the incident energy is merely redistributed amongst the different spectra.

Experimental verification of theory: The behaviour of the Bessel function when the order and the argument are varied is well known.[†] The changes in the

[†]See, for instance, Jahnke-Emde, *Tables of Functions*, Second Edition, 1933, Section XVIII.

configuration of the diffraction pattern with increasing values of v can, therefore, be readily visualised. When v is zero, we have only the central component. As v increases, the first orders begin to appear and increase in intensity while the intensity of the central component steadily falls off. The second order spectra then begin to appear. With further increase of v , a stage is reached when the first order spectra are very conspicuous, the second order spectra fairly strong and the third orders begin to appear, while the central component has nearly vanished. For still larger values of v , the second orders are stronger than the first, while the central component has reappeared and the third orders are in fair strength. Further changes of the same general nature occur for larger values of v , the spectra fluctuating in intensity, and the higher orders gaining at the expense of the lower ones.

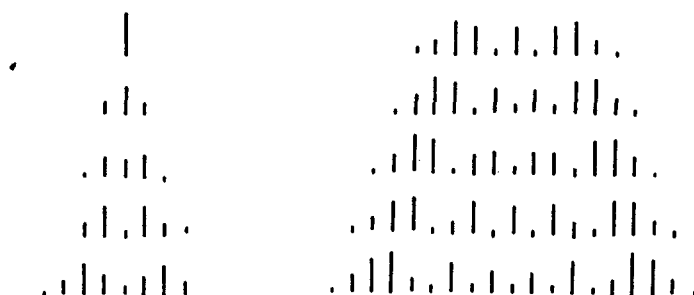
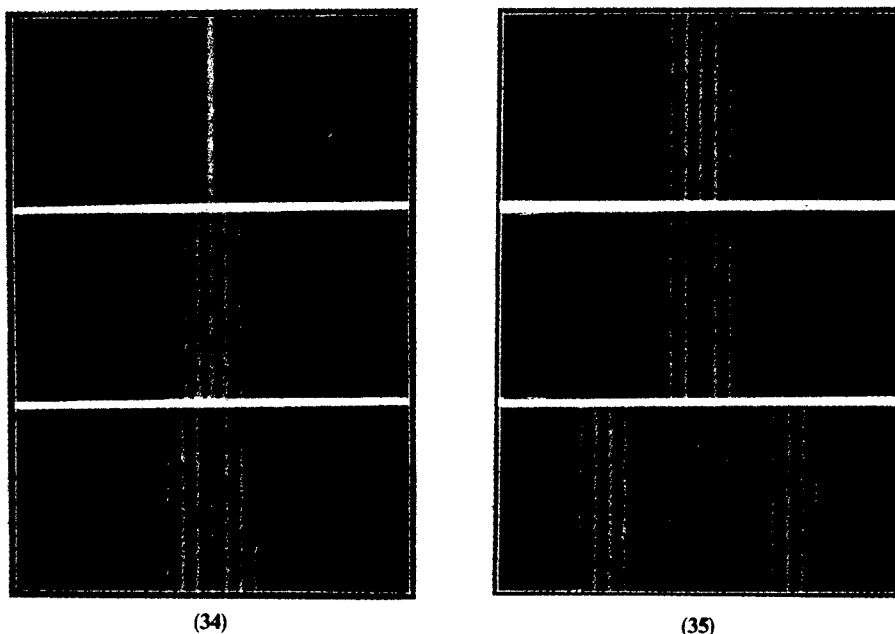


Figure 33. Relative intensities of spectra due to corrugated wave.

The relative intensities of the spectra for various values of v from 0 to 8 are represented in figure 33 which is taken from a paper by Raman and Nath,* dealing with the somewhat analogous case of a beam of light which has passed through a liquid column carrying ultrasonic waves. As will be seen from the figure, spectra of increasingly higher orders continue to appear as v becomes larger and take up the greater part of the energy, though some of the spectra of lower orders still have fair intensities. The fluctuations in the intensity of any particular order with varying v , and of the spectra of different orders with constant v are both characteristic features of the case. The disappearance of particular spectra corresponds to the zeroes of the Bessel function of the orders concerned and furnish a sharp criterion for the value of the maximum phase-retardation which is operative. It is worthy of remark that the increase in the number of spectra and consequent enlargement of the angular width of the pattern with the increasing amplitude of the ripples, as shown by figure 33, roughly correspond with the increasing divergence of the rays on emergence from

*C V Raman and N S Nagendra Nath, *Proc. Indian Acad. Sci.*, 1935, A2, 406.



Figures 34 and 35. Diffraction of light by ripples on water.

the liquid surface which is indicated in figure 32. Figures 34 and 35 reproduce a series of photographs* obtained with a ripple tank and exhibit a beautiful concordance with the theoretical results. It should be remarked that these pictures were obtained with *progressive* ripples, the boundaries of the tank being too far away to give a disturbing reflection. Theory indicates that the diffraction pattern by *stationary* ripples would be of a different character. This is readily understood, because the relative intensities of the different orders of spectra depend on the maximum retardation of phase produced by the ripples. This is a constant quantity for a progressive motion, but varies periodically with time for a stationary oscillation of the liquid surface. In the latter case, the diffraction pattern as recorded on the photographic plate would be a time average in which the special features depending on the particular value of v would have been almost completely smoothed out. It is noteworthy that in either case, the diffraction patterns can be seen without stroboscopic aid. Indeed, stroboscopic illumination would make no difference in the diffraction pattern as observed with progressive ripples. With a stationary ripple pattern, however, the diffraction pattern seen would change with the phase at which the flashes of illumination are

*D S Subbaramiah, *Proc. Indian Acad. Sci.*, 1937, A6, 333.

given. By altering this phase, it should be possible to follow the changes in the structure of the pattern corresponding to all the values of v from zero upwards to the maximum.

As the corrugation of the liquid surface produces changes of phase but no appreciable changes of amplitude in the light beam on its emergence, a microscope focussed on the surface would fail to give any indication of the existence of the ripples. When the plane of observation is moved away from the surface, however, alternations of light intensity would develop, which may be observed with stroboscopic aid for progressive ripples, and without such aid for a stationary ripple pattern. In the latter case, what we observe is an average intensity effect. The spacing of the pattern seen would therefore be $\lambda^*/2$, while for progressive ripples, the spacing would have the full value λ^* . As remarked earlier, the nature of the pattern would vary in a cyclic manner with the movement of the plane of observation. The spacing of the complete cycle is $2\lambda^{*2}/\lambda$ for a progressive wave, but if we ignore a lateral displacement of the pattern and consider only its general appearance, the period of the cycle would be one half of this, namely, λ^{*2}/λ . If, therefore, the plane of observation coincides with the liquid surface or is removed from it by a distance λ^{*2}/λ or a multiple thereof, the ripples would be unobservable, while at intermediate positions, complex patterns would be seen the nature of which depends on the amplitude of the ripples. For stationary patterns seen without stroboscopic aid, the wavelength for the average intensity effect is effectively halved, so that the period of the cycle is only $\lambda^{*2}/2\lambda$. The general theory of visibility of periodic structures including the case of ultrasonic waves of optical gratings for which $\lambda^* \gg \lambda$ has been given by Nagendra Nath.[†]

Fresnel and Fraunhofer patterns: An application of the principle that the ray-optical and wave-optical descriptions of a light-field should be completely equivalent enables us to find the effect of restricting the aperture of a beam of light in any manner. To illustrate the essential features of the problem, we consider the comparatively simple case of the passage of light through a plane diffraction grating made up of parallel strips of equal width which are alternately transparent and opaque. Exactly as in the case of a corrugated refracting surface discussed earlier, we analyse the disturbance emerging from the grating into sets of plane waves travelling in various directions, starting from the disturbance at its surface as determined by its assumed properties.

The waves incident normally on the plane grating are represented by the expression $A \sin 2\pi(vt - z/\lambda)$. At the plane of the grating ($z = 0$), this reduces to $A \sin 2\pi vt$, and we assume that this is also the disturbance emerging from the transparent strips, while over the opaque strips the disturbance vanishes. The light-field thus described is periodic over the surface of the grating with

[†] N S Nagendra Nath, *Proc. Indian Acad. Sci.*, 1936, A4, 262.

wavelength λ^* and may be therefore represented by its Fourier expansion

$$\frac{1}{2}A \sin 2\pi vt + \sum_{s=1,3,5,\dots} 2A \sin 2\pi vt \frac{\sin 2s\pi y/\lambda^*}{s\pi}.$$

We now reintroduce the co-ordinate z , and write the emerging disturbance in the form

$$\frac{1}{2}A \sin 2\pi(vt - z/\lambda) \pm \sum_{s=1,3,5,\dots} \frac{A}{s\pi} \cos 2\pi(vt - z/\lambda \mp sy/\lambda^*).$$

The first term represents the undeviated plane waves of diminished strength emerging from the grating, while the others represent a series of diffraction spectra in which the even orders are missing. These spectra appear with equal amplitudes but with opposite phases in directions equally inclined to the primary beam on either side of it. The amplitudes of the diffracted plane waves are inversely proportional to the order of the spectrum, in other words, to the sine of the angle of diffraction. Considering the situation at the edges $b = 0, \pm \lambda^*, \pm 2\lambda^*$, etc., on the surface of the screen, we notice that the diffracted plane waves traverse each of these edges in various directions but in identical phases. The diffracted disturbances may therefore be regarded as made up of sets of *cylindrical* waves diverging normally from these edges with an amplitude inversely proportional to the sine of the angle of diffraction. A similar situation also presents itself as the intermediate edges $y = \pm \lambda^*/2, \pm 3\lambda^*/2$, etc., except that the phases are now reversed. It follows that the cylindrical diffracted waves diverging from an edge have *opposite* phases according as they appear on the illuminated or the dark side of it. The diffraction spectra emerging from the grating may be considered as the result of the interferences of these cylindrical waves. On this view, the non-appearance of the spectra of even order is a consequence of the cylindrical waves from the equidistant edges being alternately in opposite phases.

The result which thus emerges, namely, that the boundary between light and shadow at the edge of a screen is a source of diffracted radiation having opposite phases on its two sides, evidently does not depend on the particular disposition of the edges in the case considered nor on their being infinitely extended or straight. It is indeed valid generally, for edges of finite length as also for curved edges. Further, the assumption that the alternate strips are completely opaque is also not essential, since a sudden transition of any kind—in amplitude or phase or both—on the two sides of a boundary of arbitrary form in a light-field would give rise to similar effects. The recognition of these consequences of optical theory is the key to an understanding of the diffraction phenomena which arise from the passage of light through apertures or its obscuration by obstacles of arbitrary form and nature. They enable us to describe these phenomena in geometric terms related to the form of the apertures or obstacles. Further, they lead us naturally to an understanding of the more recondite aspects of diffraction theory, including especially the influence of the material and thickness of the screens, and the

configuration of the edges (viz., whether they are sharp, wedge-shaped or rounded-off) on the observed phenomena.

A procedure closely analogous to that described above may be adopted to find the effect of passage of light through a single slit. We start by assuming a series of parallel slits of width a at regular intervals λ^* and then pass to the limit when $\lambda^* \rightarrow \infty$. As in the case considered above, a Fourier expansion gives the result of the passage of the light through such a grating in the form of a series. It is readily shown that this may be written in the form

$$\frac{2Aa}{\lambda^*} \left[\frac{1}{2} + \sum_{s=1,2,3,\dots} (-1)^s \frac{\sin(\pi a \sin \theta_s / \lambda)}{(\pi a \sin \theta_s / \lambda)} \right],$$

where $\lambda^* \sin \theta_s = s\lambda$. As λ^* tends to ∞ , the diffraction spectra appear in more closely contiguous directions, and their number being great, we may neglect the first term in comparison with the rest. On squaring, we obtain an expression of the familiar type for the intensity in the diffraction pattern given by a rectilinear slit. A similar expression is also obtained if we consider the diffraction pattern as the result of the interference of the cylindrical waves having opposite phases emitted by the two edges.

The validity of the treatment of diffraction problems outlined above is naturally subject to certain restrictions and in particular, depends greatly on the exactness with which the configuration and properties of any actual screen reproduce those assumed for the purpose of the Fourier analysis. It is evident also that the results of the analysis would progressively tend to deviate from the facts as the size of the structures considered approaches the wavelength of light. For, we would then actually have a terminated sequence of spectra and not an infinite sequence as assumed. These difficulties become much more acute when we consider cases in which the light is incident very obliquely on the screens or apertures.

Instead of analysing the disturbance emerging from an aperture into sets of infinitely extended plane waves, we may follow a different procedure and express it as the summation of sets of spherical waves having their origins continuously distributed over the area of the aperture. This, in fact, is the familiar approach to diffraction theory based on the principle of Huygens due to Fresnel which is generally adopted in treatises on optics. In this treatment, the intensity at any point in the light-field is expressed as a surface integral taken over the illuminated area of the aperture and then evaluated. Apart from its historic interest and its usefulness in certain cases for purposes of computation, it is evident that this classic procedure has not much to recommend it from a physical point of view. It postulates secondary sources of radiation at points of space where there are no real sources and no material particles which can serve as secondary sources. Indeed, if we examine the matter closely, we find, on carrying out the summation of the effects of the postulated secondary sources, that they disappear from the picture, leaving only secondary radiations having their origins on the boundary

of the aperture. That this is the case will be shown a little later when we consider the problem of diffraction by apertures or obstacles with curvilinear boundaries.

Diffraction by an equilateral aperture: The fundamental role played by the boundaries of an aperture in determining the physical and geometric characters of its diffraction pattern may be suitably illustrated by a simple case, namely, that of an aperture bounded by three sharp straight edges in the form of an equilateral triangle.

The light from a point source passing normally through such an aperture placed at a distance from it and after diverging further falls on a photographic plate; the pattern thus recorded with short exposures is reproduced as figure 36 and with large exposure as figure 37. Figure 38 is a greatly enlarged reproduction of the pattern recorded when an image of the light source as seen through the aperture is brought to a focus on the photographic plate by a convex lens. On comparing figure 36 and figure 38, we notice that the former exhibits trigonal and the latter hexagonal symmetry. The complete dissimilarity of the Fresnel and Fraunhofer patterns which these pictures suggest is negated by a comparative study of figures 37 and 38. We then realise that the fainter outlying parts of the Fresnel pattern which are recorded on a strongly-exposed plate present marked similarities with the features observed in the Fraunhofer patterns.

The Fresnel pattern illustrated in figure 36 and figure 37 may be completely described by the statement that in the strongly illuminated triangular area,

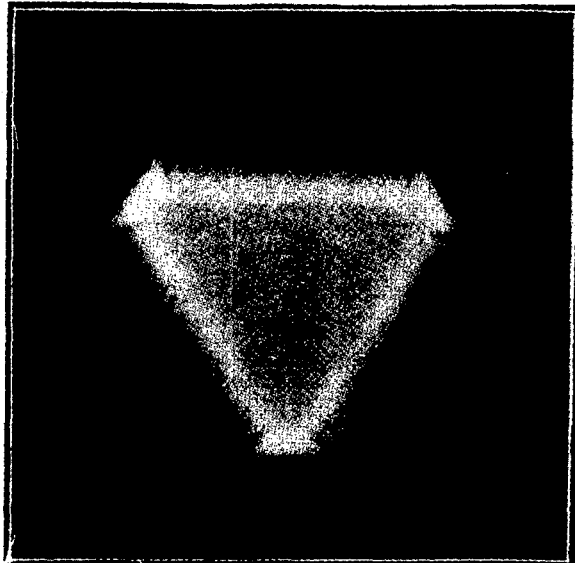


Figure 36. Fresnel pattern of equilateral aperture (weakly exposed photograph).

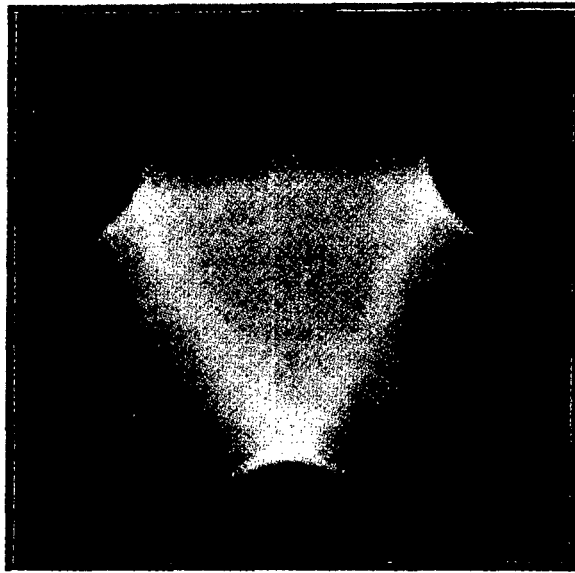


Figure 37. Fresnel pattern of equilateral aperture (strongly exposed photograph).



Figure 38. Fraunhofer pattern of equilateral aperture.

spherical waves of light passing directly through the aperture are superposed upon and interfere with the cylindrical waves diverging from each of its three edges, while in the fainter outlying regions, these cylindrical waves appear by themselves. The interference of the cylindrical waves from each edge with the primary spherical waves gives the bands of alternating intensity which are noticed running parallel to the same edge. Outside the central illuminated

area, an area of hexagonal shape is noticed where the cylindrical waves from all the three edges are seen superimposed. Further out still, we have a star-shaped hexagonal pattern where they appear superimposed in pairs; still further out, they appear individually as streamers. Running parallel to the edges of these faintly illuminated areas, we observe bands of alternating intensity which are most prominent in the vicinity of the vertices of the triangle; in this neighbourhood, they take the form of hyperbolic curves having their asymptotes normal to the sides of the triangle.

The Fraunhofer pattern illustrated in figure 38 may be described as the result of the collapse and disappearance of the central illuminated area in figure 37, consequent on the lens bringing the spherical waves which pass through the aperture to a geometric focus. In other words, the Fraunhofer pattern is due exclusively to the radiations from the edges of the aperture. Where the radiations from all the three edges are effectively superposed, we have the central hexagonal area of the pattern. Surrounding this, features are visible which are due to the cylindrical waves being superposed on each other in pairs and giving observable interferences. Further out still, the effect of each edge is observed by itself in the arms of the six-rayed star which forms the most conspicuous feature of the pattern. The rays of this star arise from the cylindrical waves diverging on either side of each edge; owing to the astigmatism of these waves, the broad streaks to which they give rise in figure 37 have contracted laterally (but not longitudinally) into the narrow streaks seen in figure 38. The fainter bands running parallel to the rays of the star are essentially similar in their origin to the bands running normal to the edges seen in the Fresnel pattern. *They arise from the interference with each other of the cylindrical waves from different parts of the same edge.* Along the central line of each ray of the star, the whole of the corresponding edge is effectively in the same phase. But when we move away from the central line, the radiations from different parts of the edge no longer agree in phase. We may then replace the line source parallel to the edge by point sources of diffracted radiation, one at each end; these give the interferences running parallel to the rays of the star. The Fraunhofer pattern may indeed with justice be described as arising from the interferences of radiations from three point sources placed respectively at the three vertices of the triangle. The amplitudes and phases of these radiations depend in a characteristic manner upon the angle of diffraction, thereby influencing the general appearance of the pattern to a notable extent.

Diffraction caustics and foci: We shall now proceed to consider the special phenomena exhibited by apertures and obstacles with *curvilinear* boundaries. It is useful in the first place to remark upon the relationship between the effects produced by an opaque obstacle and by an aperture in an opaque screen when they have the same form and situation relatively to the source of light. The illuminated areas being complementary, the sum of the effects in the two cases would everywhere be the same, being that due to the source itself. Accordingly, if

we subtract from the undisturbed effect of the light-source, that actually observed at any point in the shadow in one case, the difference would be the effect observed in the illuminated area in the other, and *vice versa*. The form of the boundary being the common feature, this reciprocal relationship indicates that we are dealing in both cases with the same physical phenomenon, namely, a diffracted radiation having its origin at the boundary. That this appears as a positive contribution in one case and as a subtractive effect in the other, or *vice versa*, is readily understood, since the boundary radiation has opposite phases on the shadowed and illuminated sides respectively.

We have now to define more precisely the character of the radiation from a diffracting edge of arbitrary form. Here again, the essential features of the case may be deduced from the simplest assumptions. Spherical waves are assumed to diverge from a point-source Q , and at a distance D from it, meet an opaque screen covering the wave-front except over an aperture bounded by a curve of arbitrary form. We represent the disturbance emerging from the aperture as a summation of spherical waves having their origins distributed continuously over its area.* Accordingly, the disturbance reaching a point P on a distant screen is written as the integral

$$\iint \frac{A}{\lambda R} \sin 2\pi(vt - R/\lambda) dS,$$

where dS is an element of area on the aperture at the point O (say), and R is the length OP . It is readily shown that

$$dS = R d R d\epsilon \cdot D/PQ,$$

where ϵ is the angle between the plane OPQ and some fixed reference plane passing through PQ . Integrating with reference to R , we obtain

$$\int_0^{2\pi} \frac{A \cdot D}{2\pi \cdot PQ} \cos 2\pi(vt - R/\lambda) d\epsilon.$$

R now signifies the distance from P of points on the boundary of the aperture and is, therefore, to be regarded as a function of ϵ . The integration with respect to ϵ from 0 to 2π may be written as an integration over a complete circuit of the boundary of the aperture; ds being an element of arc on the boundary, and ϕ the angle which it makes with the plane passing through PQ and the element, we obtain

$$\int \frac{A \sin \phi}{2\pi R \sin \theta} \cos 2\pi(vt - R/\lambda) ds,$$

*The variation of the amplitude of the assumed spherical waves with their direction of propagation is unimportant for our present purpose and is, therefore, ignored.

where θ is the angle between the incident ray reaching the element ds and the diffracted ray starting from it and reaching the point of observation. Thus, it appears that *each line-element of the boundary is a source of diffracted radiation, its strength being inversely proportional to the sine of the angle of diffraction and directly proportional to the sine of its inclination to the plane of diffraction.*

The foregoing result is quite general and may be used to evaluate the intensity in both Fresnel and Fraunhofer patterns, it being always remembered that the integral represents the disturbance originating at the boundaries of the aperture or obstacle, and does not include the undisturbed effect of the light source. The latter, if present, must therefore be added to the expression. It will be noticed that the contribution from each element of the boundary becomes large and changes sign when θ passes through zero. It is this reversal of phase of the radiation from the edge that secures the observed continuity of the illumination when we pass from the region of shadow to the illuminated region in diffraction patterns of the Fresnel type. The *amplitudes* of the radiations received at any point in the field from different parts of the edges depend principally upon the angles θ and ϕ , while their *phases* vary with R . It follows that the resultant effect would be contributed mainly by the parts of the edge for which θ is small and R is a maximum or a minimum. The latter condition automatically ensures that ϕ is $\pi/2$ or $3\pi/2$ and $\sin \phi$ is therefore numerically a maximum. Ordinarily, therefore, the diffracted radiation has its origin principally at the point or points on the edge where this runs perpendicular to the rays reaching the points of observation. If, therefore, we draw a series of normals at various points on the geometric boundary between light and shadow on the receiving screen, these normals also define the directions in which the corresponding points on the edge are most effective in diffracting light.

In the language of geometrical optics, a focus is a point at which a set of reflected or refracted rays intersect, while a caustic is a curve to which a set of such rays is tangential. These concepts may evidently be applied *mutatis mutandis* to the rays diffracted by edges in the manner discussed above. Hence, provided the edges are sharp and smooth, besides being curved, we should be able to observe diffraction foci or diffraction caustics at the points where the normals to the geometric boundary of the shadow intersect or touch each other respectively.

Perhaps the best known example of a diffraction focus is the bright spot observed along the axis of the shadow of an opaque circular disc thrown by a point source of light. A smooth spherical obstacle also gives a similar bright spot, but with a notably different colour and intensity, for reasons which we shall consider more closely later.* It is worthy of remark that the edge of a circular aperture also gives a bright spot along the axis which may be rendered visible by blocking out the superposed illumination received directly through the aperture.

*C V Raman and K S Krishnan, *Proc. Phys. Soc. London*, 1926, **38**, 350.

It should also be mentioned that an *incomplete* circular edge also gives a bright spot, though naturally of inferior sharpness and intensity.

The considerations set out above indicate that the evolute of the shadow of a curved boundary is the geometric figure along which its diffraction caustic is formed. That this is actually the case was demonstrated by observations with an elliptic boundary made by the present writer many years ago.* A circular opacity polished surface held so that it reflected light obliquely proved an excellent substitute for an elliptic aperture. Less satisfactory was a circular disc or a circular aperture with a sharp edge cut in a thin metal sheet and held obliquely. Qualitatively, the geometric evolute was found to be the locus of maximum intensity of the diffracted light. More exactly, the evolute represented the geometric limit within which the radiations from the concave part of the curved edge were concentrated. The curve of maximum intensity lay along and inside the evolute being accompanied by other and weaker interferences running parallel to it (see figure 39). These are due to the diffracted rays crossing each other at various small angles inside the evolute.

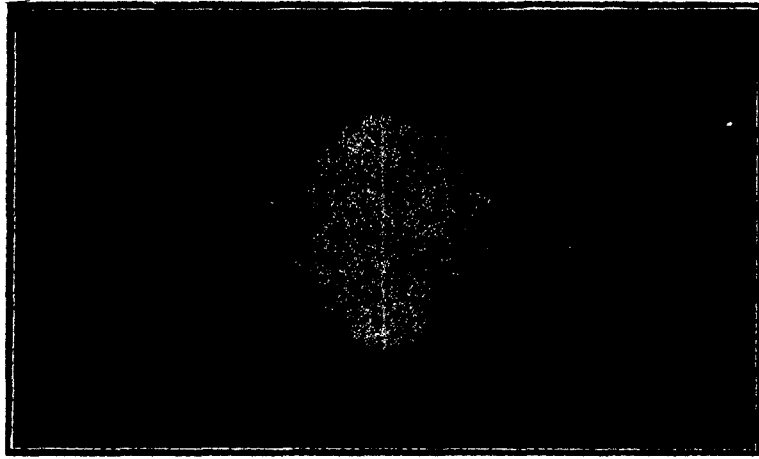


Figure 39. Diffraction caustic of elliptic aperture.

Figure 40 shows the Fresnel diffraction pattern given by an elliptic aperture in monochromatic light. The intensity in the diffraction pattern outside the elliptic area is mostly concentrated within its geometric evolute as indicated by theory. The pattern is crossed by two sets of interferences, one of them running parallel to the evolute and arising in the manner already explained, while the other set is

*C V Raman, *Phys. Rev.*, 1919, 13, 259.

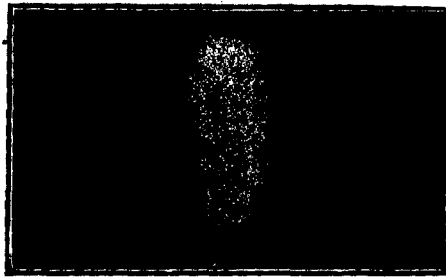


Figure 40. Fresnel pattern of elliptic aperture.

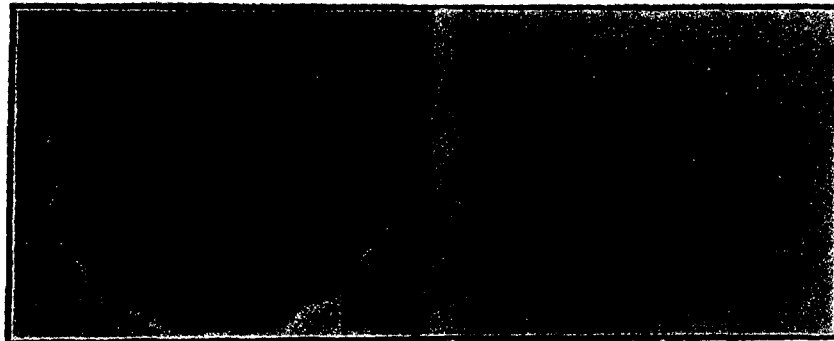


Figure 41. Diffraction by an undulating edge.

transverse to the evolute and arises from the interference of the effects due to the convex and concave parts of the edge.

Diffraction caustics are strikingly exhibited in the shadow of a disk with an undulating margin* (a nickel one-anna coin), two photographs of which taken with short and long exposures respectively are reproduced in figure 41. The diffraction pattern within the shadow which is recorded with the longer exposures follows the geometric form of the evolute of the undulating boundary. It exhibits a marked intensity at the cusps which may be regarded as foci, as well as a concentration of the luminosity along the branches of the evolute, with subsidiary interferences parallel to them. The effects in the vicinity of the cusps are very similar to those noticed when two branches of a caustic formed by refraction meet, e.g., in the case of an obliquely held transparent cylinder.†

*S K Mitra, *Philos. Mag.*, 1919, 38, 289. Other cases of interest, notably that of a disk with milled edges are illustrated in this paper.

†T K Chinmayanandam, *Phys. Rev.*, 1918, 12, 314.

The heliometer diffraction figures: The case of a semi-circular aperture has a special interest in its application to the form of the star-images seen in the heliometer; this instrument is a telescope with a divided objective, the two halves of which are capable of displacement relatively to each other along their common diameter. The case also offers an excellent illustration of the power of the geometrical method in discussing the configuration of Fresnel and Fraunhofer diffraction patterns and the relations between them. We shall here first consider the Fraunhofer pattern, and show how its geometric features may be deduced from the semi-circular form of the boundary.

We denote the angle between the incident and diffracted rays by θ , and the complement of the angle which the plane containing these rays makes with the diameter of the semi-circle by ψ . When $\psi = 0$, the plane of diffraction is normal to the diameter; the radiations from the elements of the straight edge have then the maximum amplitude, while their phases are in agreement for all values of θ . Accordingly, these radiations give a long bright streak in the pattern along a line perpendicular to the diameter. When ψ is not zero, the phases disagree, and the interferences then arising would result in alternate minima and maxima of intensity running parallel to the streak along $\psi = 0$. As in the case of the equilateral aperture considered earlier, we may regard these interferences as due to point-sources of equal strength and opposite phases placed at the extremities of the edge. When $\psi = \pi/2$, the radiations from the straight edge vanish completely.

Considering now the curved part of the boundary, the amplitude of the radiations from a line element is a maximum at the point where the edge runs perpendicular to the plane of diffraction, and diminishes gradually to zero at the points where it runs parallel to that plane. The phases of the radiations from the line elements as received in the focal plane would, on the other hand, be stationary at the former point and alter at an increasing rate as we approach the two latter points. The resultant effect of all the line-elements may, therefore, be represented by that of a source placed at the point of stationary phase, supplemented by two equal sources located at the ends of the semi-circle. These latter vanish when $\psi = 0$, but become increasingly important as ψ alters in either direction; in the limiting cases when $\psi = \pm \pi/2$, they represent the entire effect of the boundary.

Thus, in general the radiations from the straight and curved parts of the edge, taken together, may be replaced by the effect of three point-sources placed at the positions indicated in figure 42, namely, one on the curved edge and two at the corners of the aperture. The optical paths traversed by the radiations from these sources in reaching the focal plane would differ from each other by the three quantities $(\alpha + \alpha \sin \psi) \sin \theta$, $(\alpha - \alpha \sin \psi) \sin \theta$ and $2\alpha \sin \psi \sin \theta$, as will be seen from figure 42. If we denote $\alpha \sin \theta$ by ζ , the quantities ζ and ψ may be used to define the polar co-ordinates of a point in the focal plane. The interferences of the three sources, considered in pairs, would lie along the lines whose equations are

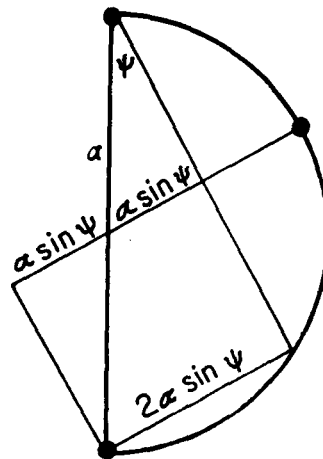


Figure 42. Diffraction by semi-circular boundary.



Figure 43. Fraunhofer pattern of semi-circular aperture.

$2\zeta \sin \psi = \text{constant}$, $(\zeta + \zeta \sin \psi) = \text{constant}$, and $(\zeta - \zeta \sin \psi) = \text{constant}$. The first equation represents the long streaks perpendicular to the diameter already mentioned, while the two latter represent sets of parabolae whose axes are *parallel* to the diameter of the semi-circle, but whose curvatures are oppositely directed with reference to the set of straight bands represented by the first equation. These features are beautifully exhibited by the photograph of the Fraunhofer pattern reproduced in figure 43. The three sets of interferences and their intersections completely determine the form of the pattern and the distribution of intensity in it.

As already remarked, the effect of the straight edge vanishes when $\psi = \pi/2$, while that of the semi-circle is equivalent to two sources placed at the ends of the diameter. The situation is then the same as for a complete circular boundary,

except that we have only one-half its effect. In other words, in the plane of the diameter, the pattern is identical with that of a complete circular aperture with the intensities reduced to one-fourth their values. When $\psi = 0$, the effect of the curved edge reduces to that of a single source placed at its midpoint; the interferences of this with the effect of the diameter would result in the straight bands due to the latter fluctuating in intensity along their length. These fluctuations diminish both relatively and absolutely, and ultimately disappear, as we move out along these bands. For, the elements of the straight edge remain in phase with each other, while those of the curved edge fall out of phase in an increasing measure as θ is increased. The effect of the latter, therefore, falls off much more rapidly than that of the former.

The line integrals over the straight and curved parts of the boundary are readily evaluated and by their summation, the intensity variations in the pattern may be found quantitatively. The former integral is

$$\int_{-a}^a A/2\pi f \cdot \sin \theta \times \cos(Z - 2\pi s \cdot \sin \psi \cdot \sin \theta / \lambda) \cos \psi \, ds$$

$$= A\alpha/\pi f \cdot \cos Z \cdot \cos \psi / \sin \theta \cdot \sin \xi / \xi,$$

where f is the focal length of the lens, ξ stands for $2\pi a \sin \psi \cdot \sin \theta / \lambda$ and Z for $2\pi(vt - f/\lambda)$. The latter integral is

$$\int_{-\psi}^{\pi-\psi} A/2\pi f \cdot \sin \theta \times \cos(Z - 2\pi a \sin \theta \cdot \sin \phi / \lambda) \sin \phi \cdot a \, d\phi.$$

When ψ is equal to $\pm \pi/2$, this reduces to

$$A \cdot \frac{\pi a^2}{f \lambda} \cdot \frac{J_1(2\pi a \sin \theta / \lambda)}{(2\pi a \sin \theta / \lambda)} \cdot \sin Z,$$

which is half the value for a complete circle. The effect of the semi-circular arc is evaluated very simply for the case when $\psi = 0$. For, the point-source to which it is then equivalent must be such that together with an equal source at the opposite end of a diameter, it should give the effect of a complete circle. Using the well known semi-convergent expansion for the Bessel function $J_1(x)$, the amplitudes and phases of the sources may be so fixed that their interferences give everywhere the required intensity.*

Comparing the photographs reproduced as figures 43 and 44 respectively, we notice that the Fraunhofer pattern has both a horizontal and a vertical axis of symmetry, while the Fresnel pattern has only the former. This is an example of the general theorem that a Fraunhofer pattern always exhibits centro-symmetry, while the Fresnel pattern has no higher symmetry than the aperture itself. The

*S K Mitra, *Proc. Indian Assoc. Cultiv. Sci.*, 1920, 6, 1.

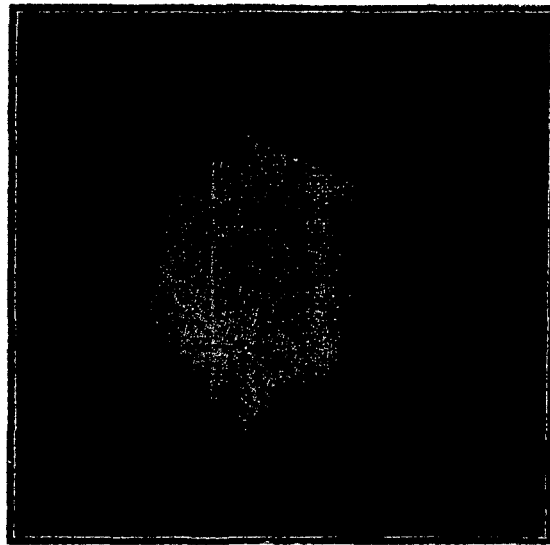


Figure 44. Fresnel pattern of semi-circular aperture.

centro-symmetry of Fraunhofer patterns is explained by the circumstance that they are due exclusively to the boundary radiations, the angle of diffraction vanishing at the centre of the pattern for all the elements of the edge; this is not the case for Fresnel patterns.

Various features are noticeable in figure 44 which may be explained by considering the radiations from the diffracting boundary and their mutual interferences. Those from the straight edge appear on both sides of the pattern as horizontal bands. Those from the curved edge are divergent on the left, but on the right converge to a focus and then diverge again. If longer exposures had been given, streamers would have been recorded diverging from the focus towards the right in various directions. The lack of symmetry of the Fresnel pattern about a vertical axis would then have been somewhat less conspicuous. The transverse bands seen in the fainter regions on both sides of the pattern arise from the interferences of the effects of the straight and curved parts of the boundary.

Diffracting apertures in the Foucault test: The general view of diffraction phenomena outlined in the preceding pages is strikingly confirmed and illustrated by the effects noticed when an illuminated aperture is observed by the aid of the light diffracted by itself. To enable this, an achromatic lens of good quality is employed to form a focussed image of a point source of light. An aperture of the chosen form is placed immediately after the lens and restricts the area of the emerging beam. After reaching a focus, the light enters a second achromatic lens which forms an image of the illuminated aperture on a distant screen. The character of this image

is found to be greatly influenced by restricting the aperture of the second lens in any manner, the size and position of the openings in the focal plane through which the light enters the second lens determining the nature of the effects observed. The phenomena noticed are readily interpreted on the view that the light forming the Fraunhofer pattern in the focal plane of the first lens has its origin on the edges of the diffracting aperture. By varying the disposition of the openings which admit the light into the second lens, effects may be exhibited which demonstrate the various characters of the edge radiation to which reference has already been made, viz., the sudden reversal of its phase in passing from interior to exterior diffraction, the dependence of its intensity on the angle of diffraction and the concentration of the intensity at special points on the edge, namely, the poles of the point of observation and sharp terminations on the edge.

When the opening of the second lens is not restricted in any manner, it gives an image of the illuminated aperture reproducing its form with full definition. A remarkable transformation of the image occurs when a small obstacle is placed at the region of maximum intensity in the Fraunhofer pattern, so as to block it out. The image then formed is a delineation of the boundaries of the aperture, the area within the boundaries appearing more or less perfectly dark. It should be remarked, however, that the edges of the aperture do not appear as bright lines in the image so formed. On the contrary, they appear as *perfectly dark lines* bordered by alternately bright and dark fringes on either side, provided the aperture of the second lens is symmetrically disposed with reference to the centre of the pattern. The reason for this fact is readily understood. As was remarked earlier, the Fraunhofer pattern is centro-symmetric by virtue of the interior and exterior diffraction by every element of the edge being of equal intensity but of opposite phases. Hence, when the light admitted into the second lens includes both interior and exterior diffraction to equal extents, the two radiations cancel each other by interference and given an image of zero intensity; the diffracted light appears in the interference fringes bordering the image of the edge on either side. If, on the contrary, the aperture of the second lens is not centro-symmetric but admits the light only on one side of the focus, this would no longer be the case. The image of the edge then appears as a *bright line* bordered by alternate dark and bright fringes.

When the second lens is completely covered except for a small opening which admits the light reaching some chosen point in the pattern, the luminosity of the edge is, in general, observed only at the poles of this chosen point. Taking, for instance, the case of a circular aperture, only two bright spots are seen, one at each end of a diameter. The intensity of these spots falls off with the increasing angle of diffraction as the opening is moved away from the focus. It is desirable that, in such observations, the opening used is not either too small or too large; in the former case the image becomes weak and diffuse, and in the latter case, the radiations from too great a length of the edge are admitted. Even when a small opening is used, the spots at the two ends of the diameter of a circular aperture

lengthen into bright arcs and finally appear as semi-circles when the opening is brought close to the focal point. In this limiting position, the edge appears brightest where it is perpendicular to the plane of diffraction and is of zero intensity where it is parallel to this plane, as required by theory. Observations of this kind serve to illustrate the geometric theory of diffraction discussed in the preceding pages. An aperture of polygonal form, for instance, exhibits a luminous point at each of its corners which brightens and merges with the luminosity of the edge observed when the opening in the focal plane lies on the corresponding streamer in the pattern. A semi-circular aperture exhibits, except in special cases, three bright spots on its boundary in the positions indicated by figure 42, the relative brightness of these spots varying greatly with the position of the opening. In the particular case when the chosen position is on the horizontal axis of symmetry (figure 43), the entire diameter appears luminous, while if it is on the vertical axis, only two bright spots are seen at the ends of the diameter, as in the case of a complete circular aperture.

Figures 45(a) and 45(b) are photographs of apertures as seen by diffracted light,

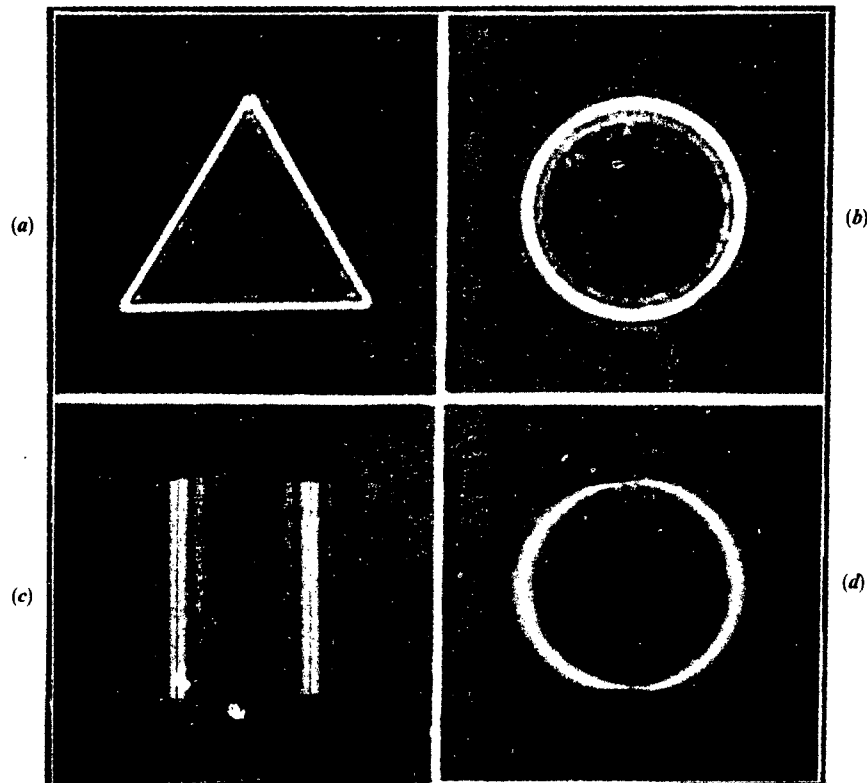


Figure 45. Diffracting apertures in the Foucault test.

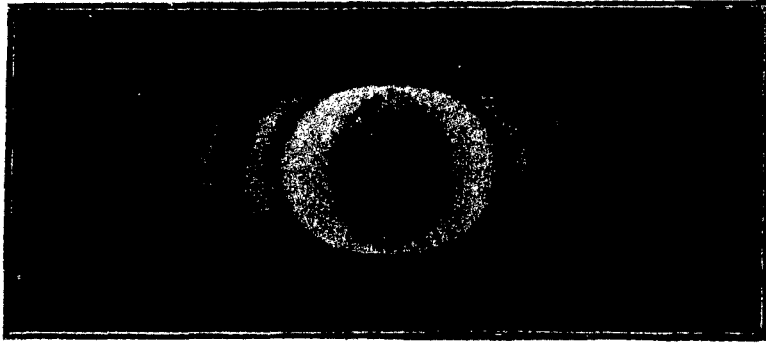


Figure 46. Circular aperture in the Foucault test.

the central rays being blocked out at the focus by a small sphere of wax; the edges appear in each case as dark lines bordered by bright lines. Figures 45(c) and 46 represent the appearance of the respective apertures when the direct rays are blocked out by a fine wire stretched across the Fraunhofer pattern through the focus. The broad fringes seen on either side of the edge in these two figures are in striking contrast with the extreme sharpness with which the geometric form of the edge itself is recorded as a dark line. These features become intelligible when it is recalled that the breadth of the diffraction fringes depends on the diameter of the wire stretched in the focal plane, while the whole effective aperture of the second lens determines the sharpness with which the edge is depicted. Figure 45(d) represents a circular aperture as seen in the usual form of the Foucault test, a knife-edge cutting off the light at the focus. It will be noticed that the edge now appears as a bright curve which is intense on the horizontal diameter and fades off towards the vertical.

The theory of the effects observed in the Foucault test is readily worked out in the relatively simple two-dimensional case* of a rectangular aperture. The light vector at any point in the focal plane of the first lens is, in this case, proportional to

$$2 \sin Z \cdot \sin (2\pi/\lambda \cdot \alpha \cdot x)/x,$$

where α is the semi-angular aperture of the opening which limits the area of the beam, and x is the co-ordinate of any chosen point in the focal plane. We consider this disturbance as effective over the aperture of the second lens, and to find the effect due to it at the focal plane of the latter, we integrate it over the area, paying due regard to the phase differences which arise between the effects due to the elements of this area when the observation is in a direction making an angle β

*Rayleigh I, *Scientific Papers*, 6, 455.

with the axis of the original light beam. The integral to be evaluated is

$$2 \int dx \cdot \sin(Z + 2\pi/\lambda \cdot \beta \cdot x) \sin(2\pi/\lambda \cdot \alpha \cdot x) \cdot /x,$$

which may be written as

$$\begin{aligned} \sin Z \left\{ \int dx \cdot \sin 2\pi/\lambda \cdot (\alpha + \beta)x/x + \int dx \cdot \sin 2\pi/\lambda \cdot (\alpha - \beta)x/x \right\} \\ + \cos Z \left\{ \int dx \cdot \cos 2\pi/\lambda \cdot (\alpha - \beta)x/x - \int dx \cdot \cos 2\pi/\lambda \cdot (\alpha + \beta)x/x \right\}. \end{aligned}$$

The integrals have to be taken between the limits x_1 and x_2 of the aperture covering the second lens. They reduce to the well known Si and Ci functions of which complete tables are available.* By assuming particular values for x_1 and x_2 , the distribution of intensity in the focal plane of the second lens may be numerically worked out. In the case of the simple knife-edge test, for example, x_2 would be taken large and x_1 small, both having the same sign. The calculations show[†] that when the edge has covered only half the central band, the luminosity at the edges of the aperture is already six times greater, and when it has covered the whole of the central band, about 80 times greater than the illumination at the centre of the aperture. The computations also show that the luminosity of the areas between the edges alternately increases and diminishes, the successive maxima becoming smaller, as the knife-edge advances. The fluctuations of colour which are observed simultaneously over the whole area of the aperture are thus satisfactorily explained. When the knife-edge traverses an ultra-focal plane of the first lens, the two edges of the aperture appear of different intensity—as is to be expected, since we are then dealing with the Fresnel pattern of the aperture.[‡] The great brightness and sharpness of the luminosity at the edges appear in these calculations as mathematical consequences of the behaviour of the Ci function which falls very steeply to an infinite negative value when its argument tends to zero. The intensity thus becomes very great in the directions $\alpha = \pm \beta$, provided x_1 is small and x_2 is large, both being of the same sign. On the other hand, when the apertures are symmetrically disposed, the Ci's being even functions of the argument cancel each other in the expressions for the intensity, while the Si's which are odd functions vanish for a zero value of the argument and reach a finite limiting value for large arguments. That the edges then appear as dark lines in the directions $\alpha = \pm \beta$ is thus readily explained, as also the sharpness of these lines when the full aperture of the second lens is operative. The case of a circular

*Jahnke-Emde, *Tables of Functions*, 1933, p. 83.

[†]Rayleigh I, *loc. cit.*

[‡]S K Banerji, *Astrophys. J.* 1918, 48, 50.

aperture can very similarly be dealt with in terms of the Si and Ci functions when the aperture of the second lens has a symmetric opening.*

Diffraction by sharp metallic edges: The edge of a razor-blade held in a beam of light is observed to diffract light through large angles, appearing as a luminous line, when viewed either from within the region of shadow or from the region of light. The light thus diffracted is found to be strongly polarised, but in perpendicular planes in the two regions. Gouy, who was the first to notice these effects, experimented with edges of various metals and discovered that both the colour of the light diffracted into the shadow and its state of polarisation depend in a remarkable manner on the material of the edge and on the extent to which it has been rounded off in the process of polishing. When viewed through a double-image prism from within the shadow, only that image of the edge appears coloured which is more intense and is polarised with the magnetic vector parallel to the edge. The second image which is fainter and is polarised with the electric vector parallel to the edge, appears perfectly white. When the incident light is polarised in any arbitrary azimuth, the diffracted light is, in general, elliptically polarised. The explanation of these phenomena will now be discussed.†

Earlier in this lecture, it was shown from theoretical arguments that the edge of an opaque screen functions as a source of cylindrical waves; these diverge both into the region of shadow and into the region of light, but in opposite phases in the two regions, their amplitude being inversely proportional to the sine of the angle of diffraction. In establishing this result, the edge was regarded as a line of discontinuity between the area in which the full effect of the incident primary waves is present and the area in which it is completely cut off. An aperture with sharp edges in a very thin sheet of metal makes a fair approach to the situation here contemplated. It should be remarked, however, that such a sheet would also reflect backwards such of the light falling on it as is not absorbed. The boundary of such an aperture is, therefore, a discontinuity in two distinct ways, firstly in respect of the light passing through it, and secondly in respect of the light reflected by the surrounding area. Diffraction effects have, therefore, to be considered arising out of these two distinct processes. The reflection of light was ignored in our earlier discussions, but if it is taken into account, the colour and polarisation effects discovered by Gouy find a natural explanation.

We shall, in the first instance, consider the case of a plane metallic screen bounded by a straight edge. Plane waves of light travelling towards the edge and incident on it in the direction $\phi = \phi_0$ (see figure 47) may be represented by the real part of the expression

$$\exp [ik\rho \cos(\phi - \phi_0) + ikt].$$

*S K Banerji, *Philos. Mag.*, 1919, 37, 112.

† C V Raman and K S Krishnan, *Proc. R. Soc. London*, 1927, A116, 254.

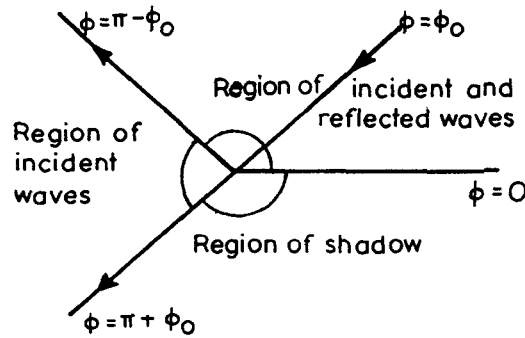


Figure 47. Reflection by half-plane.

The waves reflected by the upper surface of the screen and receding from it are given by the real part of

$$-(C_s + iD_s) \exp [ik\rho \cos (\phi + \phi_0) + ikt]]$$

or of

$$+(C_p + iD_p) \exp [ik\rho \cos (\phi + \phi_0) + ikt].$$

The complex amplitudes for the reflected wave are those characteristic of the metal for the particular angle of incidence. The alternatives refer to the cases in which the electric and magnetic vectors respectively are parallel to the edge of the screen for both the incident and the reflected waves.

We have now to find expressions for a set of cylindrical waves radiated from the edge of the screen, the superposition of which on the incident and reflected wave-trains would give in the vicinity of the planes $\phi = \pi + \phi_0$ and $\phi = \pi - \phi_0$, effects which are the same as those indicated by elementary theory, but which would be valid also for large angles of diffraction. These requirements are met if we multiply the foregoing expressions by the factor S given by the equation

$$S = \frac{\exp(i\pi/4)}{\sqrt{\pi}} \int_{-\infty}^{\sigma} \exp(-i\sigma^2) d\sigma,$$

where

$$\sigma = \sqrt{2k\rho} \cos \frac{1}{2}(\phi - \phi_0), \quad \text{for the incident waves}$$

and

$$\sigma = \sqrt{2k\rho} \cos \frac{1}{2}(\phi + \phi_0), \quad \text{for the reflected waves.}$$

It is easily verified that the resulting products are solutions of the wave-equation in cylindrical co-ordinates. S tends to different values, namely, unity and zero, when σ is positive and negative respectively and is sufficiently large. The result of the multiplication is, therefore, to restrict the appearance of the incident and reflected wave-trains to the particular regions indicated in figure 47. The

multiplier S is, however, not *exactly* unity or zero as the case may be; its *difference* from these values is given with all needful accuracy by the following expression (obtained by integration in parts):

$$\frac{\exp(i\pi/4) \exp(-i\sigma^2)}{\sqrt{\pi} \cdot 2i\sigma}$$

Substituting the values of σ in this expression and multiplying it with the expressions for the incident and reflected wave-trains, we obtain finally, by addition, the result

$$\frac{1}{4\pi} \sqrt{\frac{\lambda}{\rho}} \cdot \exp[-i(k\rho - kct + \pi/4)] \cdot \left[\frac{1}{\cos \frac{1}{2}(\phi - \phi_0)} + \frac{C_s + iD_s}{\cos \frac{1}{2}(\phi + \phi_0)} \right]$$

or

$$\frac{1}{4\pi} \sqrt{\frac{\lambda}{\rho}} \cdot \exp[-i(k\rho - kct + \pi/4)] \cdot \left[\frac{1}{\cos \frac{1}{2}(\phi - \phi_0)} + \frac{C_p + iD_p}{\cos \frac{1}{2}(\phi + \phi_0)} \right]$$

These expressions represent cylindrical waves diverging from the edge and having an amplitude varying with the direction of the observation, the angle of incidence of the light and its state of polarisation, and also dependent on the optical constants of the metal. The latter appear in the complex reflection amplitudes which are given by the formulae

$$\begin{aligned} -(C_s + iD_s) &= \frac{a - \cos \psi}{a + \cos \psi} \\ + (C_p + iD_p) &= \frac{\omega^2 \cos \psi - a}{\omega^2 \cos \psi + a}, \end{aligned}$$

where ψ is $(\pi/2 - \phi_0)$, $\omega = n(1 - ik)$ and $a^2 = (\omega^2 - \sin^2 \phi)$; n and k are the index of refraction and the absorption coefficient, respectively, of the metal. It will be seen that the cylindrical waves have large amplitudes near the boundaries of the geometric shadow and of the geometric reflection, and that the phases of the components which become large are reversed in crossing these boundaries. Further, the components bear the same relation of amplitude and phase to their respective parent waves. Their interference with these waves would, therefore, correctly describe the diffraction fringes observed in the vicinity of these boundaries. The expressions being also valid for the large angles of diffraction, they contain within themselves the explanation of the experimental facts concerning the intensity, colour and state of polarisation of the light diffracted by sharp edges.

The foregoing treatment of the problem of diffraction by a straight edge is based upon Sommerfeld's solution for the physically unrealisable case of a perfectly reflecting half-plane, but differs from it in taking the actual properties of the screen into account. It might be remarked that a metallic knife-edge is more

appropriately regarded as a wedge than as a half-plane. The theoretical expressions (due to Poincaré and others) for a perfectly reflecting wedge may, however, be modified in the same way by considering the actual reflecting power of the material of which it is made. Taking the wedge to be bounded by the surfaces $\phi = 0$ and $\phi = \chi$, the edge effect is given by formulae similar to those for a half-plane, $1/4\pi$ being replaced by $\sin(\pi^2/\chi)/2\chi$, and the expressions within the square brackets by

$$\text{or by } \left[\frac{1}{\cos \frac{\pi(\phi - \phi_0)}{\chi} - \cos \frac{\pi^2}{\chi}} - \frac{C_s + iD_s}{\cos \frac{\pi(\phi + \phi_0)}{\chi} - \cos \frac{\pi^2}{\chi}} \right]$$

$$\left[\frac{1}{\cos \frac{\pi(\phi - \phi_0)}{\chi} - \cos \frac{\pi^2}{\chi}} + \frac{C_p + iD_p}{\cos \frac{\pi(\phi + \phi_0)}{\chi} - \cos \frac{\pi^2}{\chi}} \right]$$

as the case may be. Writing $\chi = 2\pi$, we immediately regain the preceding expressions for a half-plane.

The new feature introduced by considering the optical properties of the screen is that the edge radiation appears as a summation of two distinct effects. For normal incidence ($\psi = 0$), the components due to reflection are numerically identical but are different in sign for the two possible states of polarisation. If, therefore, the incident light be unpolarised, the light diffracted through large angles would be partially polarised, and this effect would be most marked in directions nearly parallel to the surfaces of the screen or wedge, since the quantities added or subtracted would then be nearly equal numerically. The electric vector parallel to the edge would be the stronger component in the region of light or exterior diffraction, and would be the weaker component in the region of shadow or interior diffraction.

The incident light being white, the colour of the radiation diffracted by the edge would be determined by two considerations. The wavelength appears as a factor in the expression for the intensity, and thus would tend to make the diffracted light reddish, irrespective of the state of polarisation of the incident radiation. The colour would also be influenced, and in quite a different way, by the appearance of the optical properties of the metal explicitly in the expressions. Since the amplitudes of reflection occur with opposite sign in the two cases, the wavelengths strengthened in one case will be weakened in the other, and *vice versa*. Thus, in the region of shadow, the colours for which the reflecting power of the metal is greater would appear strengthened in the electric vector perpendicular to the edge and weakened in the electric vector parallel to the edge. This effect would increase with the angle of diffraction, so much so that the favoured colours would become more and more marked in one component, and less and less marked in the other component, the further we proceed into the

region of shadow. Similar effects should occur in exterior diffraction, but with the parallel and perpendicular components exchanging places in respect of both colour and polarisation.

If the incident light be plane-polarised in an azimuth inclined to the edge, the diffracted light would exhibit a rotation of the plane of polarisation as well as ellipticity, the latter appearing as a consequence of the change of phase in metallic reflection. From what has already been remarked about the effects observed when the incident light is unpolarised, it follows that both the rotation and ellipticity would depend on the nature of the screen, and in the case of strongly coloured metals would be notably a function of the wavelength of the light. The determination of these two quantities gives us both the ratio of intensities of the parallel and perpendicular components and the difference of phase between them, and would, therefore, enable a more stringent test of the theory to be made than would be possible when incident unpolarised light is employed.

The results of the foregoing theory are in general agreement with the original observations of Gouy. Quite recently, the subject has been very carefully investigated by M Jean Savornin,* in whose memoir will be found also a complete bibliography of the subject and a detailed discussion of the earlier results of other workers. Savornin has quantitatively studied the phenomena and compared them with the results expected theoretically on the assumption that the screens are perfectly conducting half-planes or wedges, as also according to the modified formulae in which the optical properties of the material are taken into account. The evidence is decisively in favour of the latter procedure. Indeed, Savornin's data for the variation with the wavelength of the rotation of the plane of polarisation and the ellipticity of the light diffracted by a razor edge, and by the same when covered with gold by cathodic deposition, show such a striking resemblance with the curves deduced from the theory and the known optical properties of steel and gold respectively, as to leave no room for doubt of the essential correctness of our formulae. The ellipticity for a steel edge is found to be small and to diminish towards the red end of the spectrum, while the rotation increases at the same time, though only slowly. In the case of gold, the ellipticity shows a pronounced maximum at about 5,200 A.U., dropping off to smaller values at both smaller and longer wavelengths, while the rotation exhibits a minimum at about 4,900 A.U., and rises very steeply towards the red end of the spectrum. These observations are in full accord with the indications of our theory.

The formulae are equally successful in other respects. They completely explain the striking difference in colour of the two components of the diffracted light. They account for the rapid increase in the rotation of the plane of polarisation and in the ellipticity produced by tilting the plane of the diffracting edge away from the symmetric position in one direction or the other, the deviation of the

*J Savornin, *Ann. Phys.*, 1939, 11, 129.

diffracted rays remaining constant. They also explain in a quantitative manner the variation of these quantities and of the intensity of the diffracted light with the angle of diffraction. In making the comparison between theory and experiment, it is necessary to consider not only the optical constants of the material, but also the angle of the wedge, since the latter is found to influence the results very markedly, especially when this angle is at all considerable. It is also necessary to remember that the theory is strictly applicable only in the case of a perfectly sharp and straight edge—a state of affairs to which the observations show that a fresh razor blade may be a remarkably good approximation. It may be mentioned that the optical phenomena exhibited by such an edge are so striking and so easily observed that they should be personally familiar to every student of optics.

Diffraction by semi-transparent laminae: As is well known, metals are ordinarily opaque to light, but in extremely thin layers transmit light. By cathodic deposition, or preferably by evaporation in vacuum, it is possible to obtain metal films of controlled thickness and consequently of any desired degree of transparency. By protecting part of the surface of a plate of glass or quartz by a razor edge held obliquely in contact with it, it is possible to coat the plate with a metallic film partially transmitting light and terminating in a straight edge,* leaving the rest of the plate clear. The same technique is also applicable for obtaining non-metallic films by evaporation in vacuum. The diffraction patterns of the Fresnel class due to semi-transparent laminae bounded by a straight edge exhibit interesting features not observed either with opaque screens or with transparent laminae. In the familiar diffraction pattern due to an opaque screen with a straight edge, we have a few fringes of rapidly diminishing visibility running parallel to the edge in the region of light, and a continuous illumination falling off steadily to zero intensity in the region of shadow. A semi-transparent film, on the other hand, exhibits a great number of interference fringes in the region of shadow, besides the fringes of moderate visibility in the strongly illuminated region. As the thickness of the film is increased and its transparency thereby diminished, the first few fringes in the region of shadow become less clear, while the subsequent ones gain visibility in spite of the diminished intensity of light in the field. The fringes having the maximum visibility move further into the region of shadow with increasing thickness of the film, until ultimately they disappear altogether. Another interesting feature is that the appearance of these patterns alters greatly with the colour of the light. This is a consequence of the marked variation of the transparency of the films with the wavelength.

Figure 48 reproduces the Fresnel fringes due to the edge of a semi-transparent silver film. To enable the effects observed on both sides of the edge to be seen simultaneously, a photometric wedge was set across the pattern when it was

*N Ananthanarayanan, *Proc. Indian Acad. Sci.*, 1939, A10, 477.

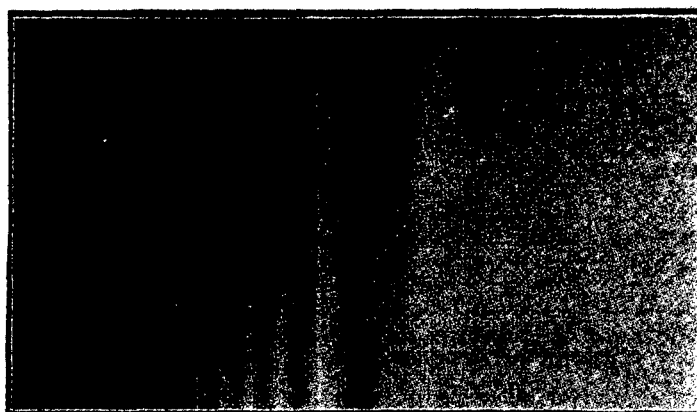


Figure 48. Diffraction by a thin metallic half-plane.

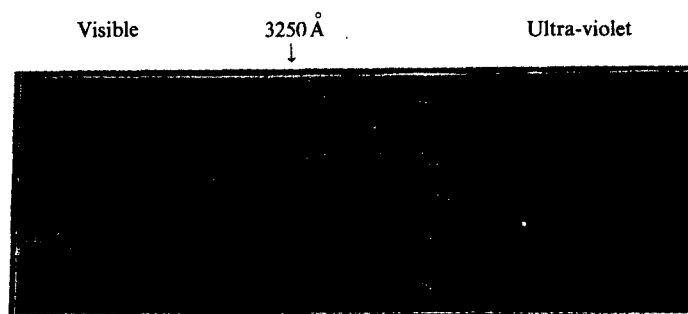


Figure 49. Diffraction by silver in the vicinity of 3250 A.U.

photographed. The fringes of low visibility on the strongly illuminated side, and the numerous fringes of high visibility in the shadow were thus recorded respectively in the upper and lower parts of the photograph. To exhibit the changes in the pattern with wavelength, the fringes may be set transversely on the slit of a spectrograph. The dispersion by the instrument then indicates how the position and intensity of the fringes alter with wavelength. Silver has a region of comparative transparency in the near ultra-violet at about 3,250 A.U. The measurements by Minor show that the optical constants n and k change rapidly in the vicinity of this band, n falling steeply and k rising equally rapidly with increasing wavelength. The influence of these changes on the configuration of the diffraction fringes is shown by the spectrogram reproduced in figure 49. A marked displacement of the fringes on the two sides of the band at 3,250 A.U. and

their practical disappearance inside it are the notable features revealed by this record.*

The phenomena described above become intelligible when we regard the Fresnel pattern as arising from the interference of the cylindrical waves having their origin at the edge of the film with the plane waves regularly transmitted on either side of it. The high visibility of the interferences observed in the region of shadow is a consequence of the light transmitted by the film and that diffracted by the edge being of comparable intensity. The thicker the film, the further we have to move into the region of shadow for this situation to occur, while both nearer and still farther, the interfering waves differ greatly in amplitude, thereby diminishing the visibility of the resulting fringes. The positions occupied by the maxima and minima of intensity depend on the geometrical differences of path between the interfering plane and cylindrical waves, due correction being made for their initial phase-difference, and especially for the change in phase of the light transmitted through the film. These considerations also serve to explain the remarkable variations in the positions and visibility of the fringes noticed in figure 49 as we pass along the spectrum, and especially in the vicinity of the band of transparency at 3250 A.U.

By exposing a silver film having a sharp edge to the action of iodine,[†] it may be completely converted into a film of silver iodide which transmits the red end of the spectrum freely, but is nearly opaque at the violet end. Figure 50(a) reproduces the Fresnel pattern given by such a film in red light. Its approximately symmetrical character indicates that it arises, at least in part, from a difference in phase between the waves transmitted on either side of the edge. Figure 50(b) which reproduces the Fresnel pattern observed in violet light is a striking contrast. Here, the part covered by the film appears as in deep shadow; the photographic exposure necessary to record the fringes seen resulted in those of low visibility appearing in the strongly illuminated part of the field being effaced by over-exposure. Figure 50(c) is the Fresnel pattern of a somewhat thicker and therefore less transparent film in red light; this shows the fringes more clearly on one side than on the other. Figure 50(d) illustrates the importance of a sharp edge by exhibiting the effect of its absence on the Fresnel pattern due to a film of Canada balsam; it will be noticed that the fringes have completely disappeared from one side and show rapid changes in visibility on the other side. This is the result of the film sloping off at its termination instead of having a sharply-defined edge.

Colours of the striae in mica: As is well known, mica has a perfect cleavage, and the sheets obtained by splitting the mineral exhibit a remarkable uniformity of thickness, as is shown, for instance, by the perfection with which they exhibit

*N Ananthanarayanan, *Proc. Indian Acad. Sci.*, 1942, A14, 85. The photographs reproduced in figure 50 are also from his work.

[†]A tiny crystal of iodine placed on a silver film gives beautiful rings of colour.

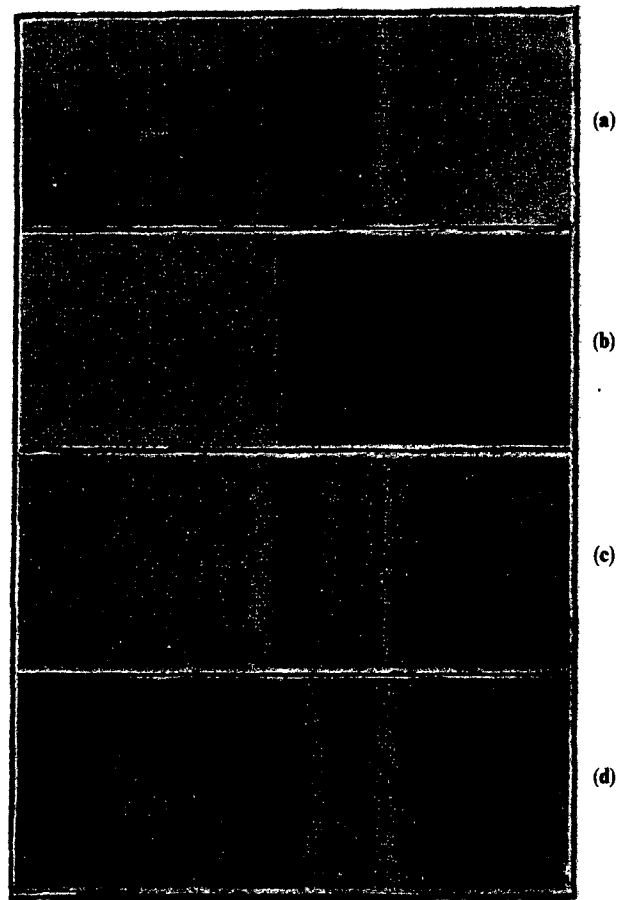


Figure 50. Fresnel patterns of semi-transparent laminae.

Haidinger's rings, and by the uniform colour and brightness of large areas of the surface of the sheet as seen by the reflected light of a mercury lamp. Whenever a variation of brightness or colour appears, it is sudden, indicating a sharply defined boundary at which a change of thickness occurs. These changes of thickness become vividly apparent when the mica is examined by the method of the knife-edge or Foucault test. They then appear as *bright* lines, often exhibiting brilliant colours.* Observed in the same test but with a symmetrical aperture, the striae are seen as *dark* lines bordered by bright coloured fringes on either side,

*C V Raman and P N Ghosh, *Nature (London)*, 1918, **102**, 205; see also P N Ghosh, *Proc. R. Soc. London*, 1919, **A96**, 257.

indicating a reversal of phase of the edge waves analogous to that we have already noticed in the case of other diffracting boundaries (see figure 51). Microscopic examination shows that the laminar boundaries may be single or multiple.* and the phenomena which the striae exhibit are found to depend on their precise nature in this respect. Single striae are extremely sharp laminar edges and are, therefore, well suited for a critical study of the diffraction effects due to such edges. They diffract light through large angles[†], exhibiting colour and polarisation effects which, in some respects, are analogous to and in other respects differ from those observed with sharp metallic edges. Examined by direct light in critical focus under high powers of the microscope, the edges appear as dark lines bordered by bright fringes,[‡] but as we shall see presently, the observed facts are not reconcilable with elementary notions of diffraction theory. These circumstances lend interest to a detailed study of the phenomena and justify an attempt to explain them on the basis of more exact theory.[§]

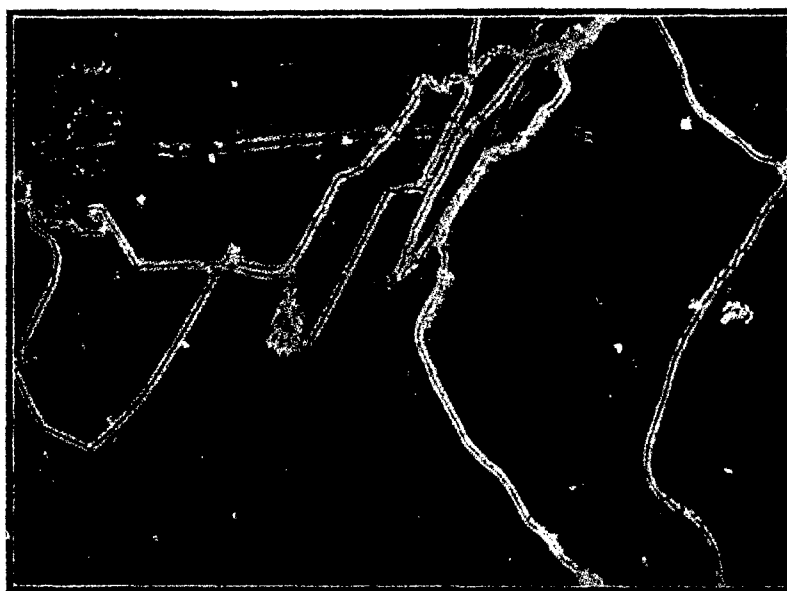


Figure 51. Mica striae in the Foucault test.

*P N Ghosh, *Proc. Indian Assoc. Cultiv. Sci.*, 1920, 6, 51.

†I R Rao, *Indian J. Phys.*, 1928, 2, 365.

‡N K Sur, *Proc. Indian Assoc. Cultiv. Sci.*, 1922, 7, 125.

§C V Raman and I R Rao, *Proc. Phys. Soc. London*, 1927, 39, 453.

When a sheet of mica is held in the path of a beam of light and the field of view behind it is examined through a lens, the striae render themselves evident by the diffraction fringes of the Fresnel class to which they give rise. From the character of these fringes, it is evident that they arise principally from the difference in phase of the waves transmitted on either side of the boundary, though the difference in amplitude consequent on the difference in thickness also requires consideration. The central fringe in the Fresnel pattern is often brightly coloured. If, however, the difference in thickness be considerable, no colour is noticed, but the central fringe then appears darker than the rest of the field. When the slit of a pocket spectroscope is set transversely across the pattern, alternate dark and bright bands may be seen running obliquely through the spectrum at the centre of the fringe system. The bright bands determine the colour of the central fringe and if their number is not too great, it may be noticed that they correspond to the wavelengths at which the outer diffraction fringes are very weak. These oblique bands in the spectrum indicate that the position of the central dark fringe shifts laterally with the change of wavelength. Using white light and a stria giving a sufficiently large path difference, this asymmetry averages out and should cease to be evident in the absence of spectroscopic aid. In practice, however, the fringes are often more prominent on one side of the pattern than on the other. There is little doubt that this is due to a disturbing factor, namely, the finite width of the striae. Instead of a single sharp edge, we have a series of them like an echelon. In such a case, the diffraction fringes are stronger on the retarded side of the wave-front than on the other, a circumstance which is readily understood if we consider the form of the wave-front after its passage through the echelon.

The Foucault test is the most suitable way of examining the light diffracted by the striae at comparatively small angles with the primary beam. The colours exhibited are complementary to those observed in the central fringe of the Fresnel patterns, and the changes produced by tilting the plane of the mica with reference to the incident light are also of a complementary character in the two cases. Thick striae appear white in the Foucault test. Spectral examination, however, which discloses an alternation of intensity with wavelength. This is readily explained, as the difference in phase of the waves transmitted on either side of the boundary would have a maximum effect when it represents an odd number of half wavelengths and would have no effect when it represents an integral number of wavelengths; only the small differences in amplitude would then be left to give any observable diffraction effect, according to the elementary theory.

For examining the light diffracted at larger angles, it is convenient, as in the case of metallic edges, to illuminate the stria and view it through a low-power microscope focussed on it. It then appears as a bright line exhibiting colour, but the latter is found to alter with the angle of diffraction in a manner which depends on the character of the stria, viz., the phase-retardation on the two sides of the boundary and its micro-structure. The most striking and interesting results are those shown by single striae. Seen in a direction nearly coinciding with the

incident light, the colour is the same as when it is observed in the Foucault test, viz., complementary to the colour of the central fringe in the Fresnel pattern. But on tilting the microscope away from this direction, the colour alters in a continuous sequence which is not symmetrical with respect to the direction of the incident light. The stria is brighter when viewed from the retarded side of the wave-front, but the colours are more striking on the other side; the stria appears achromatic when viewed rather obliquely from the retarded side of the wave-front.

It is found that the light diffracted by the individual striae is partially polarised. The percentage of polarisation increases with increasing angle of diffraction, the electric vector of the favoured component being *perpendicular* to the edge on the retarded side of the wave-front and parallel to it on the other side. The partial polarisation is, however, less marked on the retarded side of the wave-front, while on the other side, it is easily observed and in some cases is found to be nearly complete at an angle of diffraction of 90° . A quantitative comparison with the case of a steel razor blade shows, however, that the radiation by the laminar boundary is less perfectly polarised. Examination by a double image prism shows that the two images of the striae may exhibit a difference in colour as well as of intensity. More detailed studies of this effect and of the elliptic polarisation to be expected when the incident light is polarised in any azimuth are, however, lacking.

The visibility of the striae under the high powers of the microscope is a consequence of their being extremely sharp boundaries which diffract light. Under low powers, the mica striae appear as bright lines on a dark ground when viewed under oblique illumination and as dark lines on a bright ground when seen in direct light. The diffraction of light by a stria and its visibility under the microscope are thus closely connected. The stria, seen by direct light and out of focus, exhibits the usual Fresnel pattern. If the retardation be not too great, this has a coloured centre, and the fringes on either side of it have a spacing which progressively diminishes from the centre outwards. As the focus is approached, the fringes become narrower, and the character of the pattern also alters. At critical focus the stria appears as a perfectly black line with equally spaced dark and bright fringes bordering it, these being often more numerous and distinct on the thicker side of the stria than on its thinner side. To investigate whether this pattern is influenced by the phase difference on the two sides of the edge, a monochromator may be used as the light source, and the wavelength continuously varied. The surprising and interesting observation* is then made that apart from a narrowing down of the fringes with diminishing wavelength, the nature of the pattern *as seen at critical focus* does not notably alter as the wavelength of the light is changed over the whole range of the spectrum from red to violet (see figure 52). On the other hand, the Fresnel patterns of the same striae

*Previously unpublished observation by the author.

when seen out of focus show striking changes, appearing very prominently at some wavelengths, and nearly disappearing at the other lengths, these being different again for the different striae (see figure 53). It thus appears that the phase-relation of the wave-fronts on the two sides of a stria does not notably

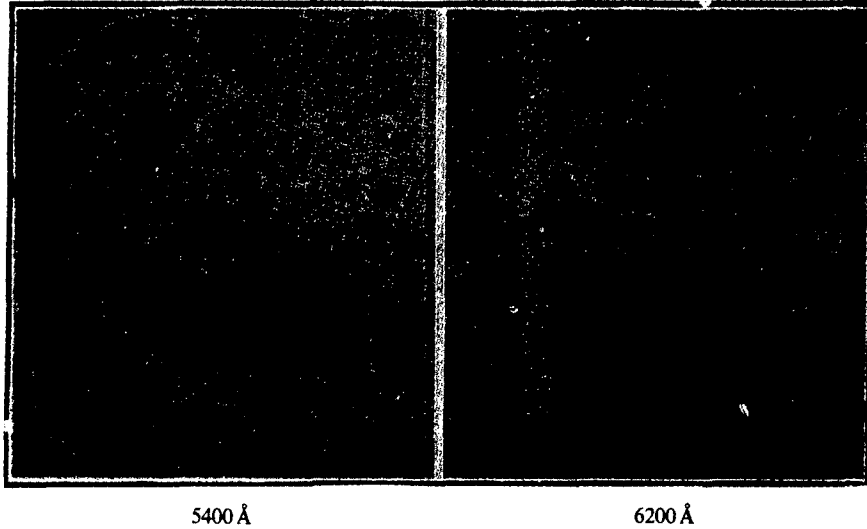


Figure 52. Mica striae in the microscope (in focus).

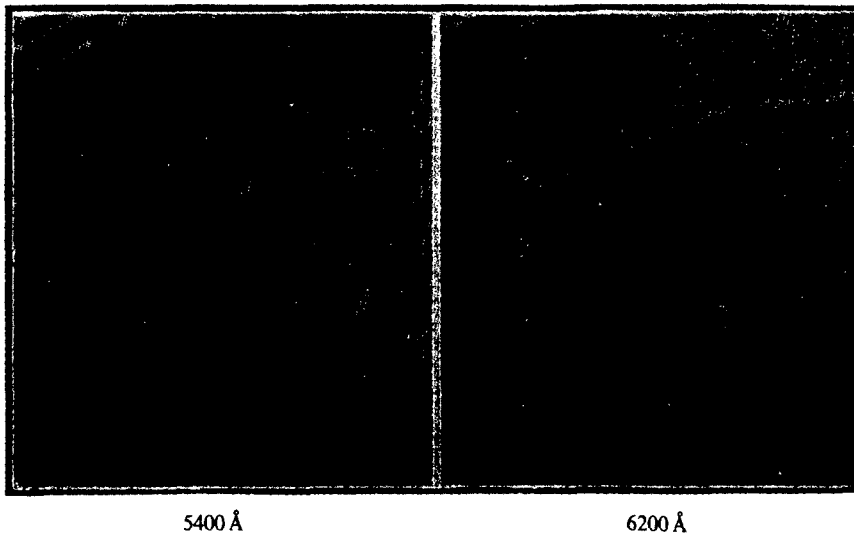


Figure 53. Mica striae in the microscope (out of focus).

influence its microscopic aspects when seen in focus, and that the latter depends on the actual difference of thickness of the mica on the two sides of the stria and on its unresolved micro-structure. The asymmetry of the diffraction pattern at critical focus appears to be variable. In some cases, hardly any fringes are seen on the thinner side of the mica, while in others, several may be seen, though generally fewer than on the thicker side.

Very significant also are the effects noticed when the microscope is put *slightly* out of focus one way or the other. In the case in which the pattern at critical focus is strongly asymmetrical, it is found that when the microscope objective is slightly pushed towards the mica, a bright band of light forms on the thicker side of the pattern and moves into the thinner side. This effect is analogous to the well known Becke phenomenon, and the observations indicate that it is a consequence of the unsymmetrical diffraction of light through large angles by a laminar boundary, for which direct evidence is forthcoming, as already set out. The nature of the pattern seen at critical focus also alters and in an unsymmetrical way when the incidence of the light on the mica is made oblique. The fringes crowd up towards one side of the edge, becoming very fine and numerous and remaining well-defined, while on the other side, they recede from the edge, and become fewer, broader and more diffuse. The effects are reversed when the incidence is altered from one side to the other, the fringes being better seen in either case when they are on the thicker side of the mica.

It is evident from the observed polarisation of the light diffracted through large angles, the variations of its colour and intensity and especially from the microscopic phenomena described above, that a theory of laminar diffraction which considers only the differences in phase and amplitude of the waves transmitted on either side of the boundary can, at best, give only a very imperfect account of the phenomena. By proceeding somewhat on the same lines as those adopted in the case of sharp metallic edges earlier in this lecture and considering also the waves reflected at the boundary, the position may be somewhat improved. In particular, we may get at least a general indication of the nature of the polarisation effects to be expected. Such a treatment, however, fails to explain the *asymmetry* with respect to the direction of the incident rays which is an essential and important feature in the observations. It is evident, therefore, that a satisfactory theory of laminar diffraction is, as yet, lacking.

Talbot's and Powell's bands: These bands are observed with white light in a spectroscope under certain conditions when one half of the aperture of the instrument is covered by a retarding plate. The theory of these bands accordingly depends on the nature of the Fraunhofer diffraction pattern due to a rectangular aperture, one half of which is covered by a retarding plate. This is evidently the same as the pattern due to the separate halves of the aperture, but modified by their mutual interference. The intensity in the pattern may be found in the usual way by integrating over the area of the aperture, and comes out (omitting a

constant factor) as

$$4a^2 \frac{\sin^2 \eta}{\eta^2} \cdot \cos^2 (\delta - \eta),$$

where $\eta = \pi a \sin \theta / \lambda$, a being the half width of the aperture, θ the angle of diffraction, and 2δ the retardation produced by the plate. In the particular case when δ is zero or any multiple of π , the pattern is identical with that of the complete aperture of width $2a$. More generally, the pattern is crossed by the interference bands expressed by the factor $\cos^2 (\delta - \eta)$, the values of θ for which the resulting intensity is zero being given by

$$\sin \theta = (\mu - 1)t/a - (n + \frac{1}{2})\lambda/a,$$

t being the thickness of the retarding plate and μ its refractive index. The angular separation of the interference bands is thus inversely proportional to the aperture. Considering the particular interference band appearing within the central fringe of the pattern, the shift of its angular position with a change of wavelength $d\lambda$ is given by

$$\lambda \frac{d\theta}{d\lambda} = - \left(\mu - 1 - \lambda \frac{d\mu}{d\lambda} \right) t/a,$$

and is thus proportional to the thickness of the plate and inversely proportional to the aperture.

This shift of the interference fringes with wavelength may be exhibited by setting the focussed pattern for white light *transversely* on the slit of a spectrograph. The interferences then appear as bands *obliquely* traversing the spectrum,* one such band being visible within the central fringe at any given wavelength (see figure 54). The inclination of the interference bands to the direction of the spectrum is determined by the ratio of the shift $d\theta/d\lambda$ parallel to



Figure 54. Spectral analysis of laminar diffraction.

*N K Sethi, *Phys. Rev.*, 1920, 16, 519.

the slit and of the shift $d\psi/d\lambda$ perpendicular to it due to the dispersion of the instrument. The separation of the successive interferences along the spectrum is determined by the quantity

$$\lambda/d\lambda = \left(\mu - 1 - \lambda \frac{d\mu}{d\lambda} \right) t/\lambda = -a \frac{d\theta}{d\lambda},$$

and is thus inversely proportional to the thickness of the plate. If $\lambda/d\lambda$ exceeds the resolving power of the spectrograph, the bands would naturally cease to be observed. The visibility of the interferences produced by a thick retarding plate thus provides a test of the resolution available. It can easily be arranged that the retardation giving the diffraction pattern arises from the difference of the refractive indices of two media. For instance, a glass plate of thickness t and refractive index μ_g may be immersed in a cell of liquid of refractive index μ_l covering half the aperture; the path retardation would then be $(\mu_g - \mu_l)t$ and the shift of the interferences with wavelength would be given by

$$\lambda \frac{d\theta}{d\lambda} = - \left[\left(\mu_g - \lambda \frac{d\mu_g}{d\lambda} \right) - \left(\mu_l - \lambda \frac{d\mu_l}{d\lambda} \right) \right] t/a.$$

Thus, when the fringes given by this arrangement are set transversely on the slit of a spectrograph, whether the interference bands in the spectrum slope up or slope down, is determined by the sign of the difference between the quantities $(\mu - \lambda(d\mu/d\lambda))$ for the two media which are their group refractive indices and not by the difference of their wave refractive indices μ . Only at the particular wavelength for which the group indices for the glass and the liquid are the same, would the fringes run horizontally in the spectrum. On either side of this wavelength, the bands would slope in opposite directions (see figure 55).

If the central fringe of the diffraction pattern in white light is set on the spectrograph *parallel* to the slit and not transversely, the interference bands would now appear crossing the spectrum in the direction of the slit. Their

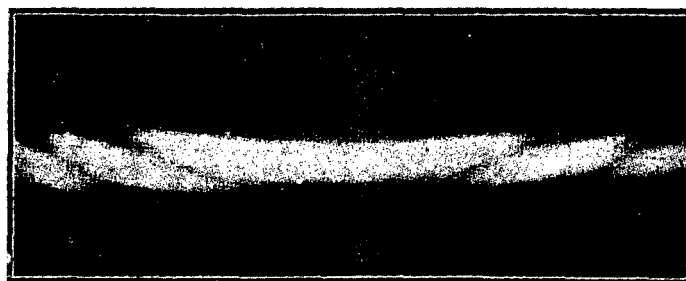


Figure 55. Spectral analysis of laminar diffraction.

separation along the length of the spectrum would, however, be the same as before, and their visibility would be subject to the same condition, namely, the sufficiency of the resolving power of the instrument. If now the slit of the spectrograph is opened wide, very remarkable changes would be noticed in the visibility of the interferences, depending upon which side of the aperture forming the diffraction pattern is covered by the retarding plate.* In one position of the retarding plate, the visibility of the fringes in the spectrum rapidly diminishes to zero when the slit is opened and after some feeble reappearances finally vanishes. In the other position of the retarding plate, the slit may be opened wide, and though this necessarily diminishes the purity of the spectrum, the interference bands continue to be seen in it, and indeed in favourable cases suffer no diminution in their visibility. These results are readily understood when we consider the two directions of march of the interferences, proportional respectively to $d\theta/d\lambda$ and $d\psi/d\lambda$ which are superposed in the spectrum. In one position of the retarding plate, these movements are in the same direction. Hence, the displacements are added and at any given point of the spectrum, the maxima and minima of illumination are superposed to an increasing extent with the opening of the slit. The rapid diminution of the visibility to zero after minor reappearances follows as a necessary consequence. In the other position of the retarding plate, the two directions of march of the fringes are opposed and if they are numerically equal, compensate each other. The interferences, therefore, remain fixed in the spectrum and suffer no diminution in their visibility when the slit is opened wide.

The distribution of intensity in the central fringe of the pattern is shown in figure 56 for a series of values of δ and exhibits the lateral movement of the interferences by the slope of the line $A_1 A_2 A_3 A_4 A_5$ joining the zeroes of illumination in the successive curves. If, as remarked above, this slope is exactly compensated by the dispersion of the spectrograph, the interference fringes are rendered stationary and are, therefore, seen with perfect visibility. From the diagram it is also evident that if the dispersion of the spectrograph is diminished to about one-half of that required for such perfect visibility, the minimum A_5 in the fifth curve would be superposed on the maximum B_1 of the first curve, and the visibility of the fringes would, therefore, be completely destroyed. On the other hand, if the dispersion is greater than that required for perfect visibility, the straight line drawn through the minimum A_5 would slope over to the left and traverse the region outside the central fringe where the intensities are much smaller. The interferences would, therefore, continue to be visible in the spectrum though with diminished visibility.

It may be remarked that the foregoing discussion practically covers the theory of Talbot's and Powell's bands. We have only to remark that in the usual form of

*N K Sethi, *Philos. Mag.*, 1921, 41, 218.

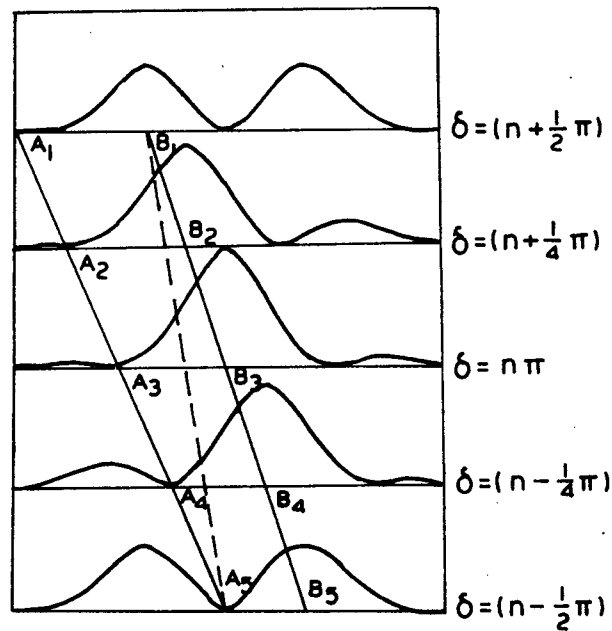


Figure 56. Graphs of function $(\sin^2 \eta/\eta^2) \cos^2(\delta - \eta)$.

these experiments, the retarding plate is inserted within the spectrograph, which itself simultaneously forms the diffraction pattern and disperses it into a spectrum. The conditions for obtaining Talbot's bands under these conditions immediately follow from the foregoing theory and may be stated very simply. *The visibility of Talbot's bands is perfect when the resolving power of the spectrograph at full aperture is twice the minimum required for separating the bands. The bands are invisible when the resolving power of the instrument is only sufficient to separate them.* The conditions for observing the bands are much more flexible in the form of the experiment discussed above in which the laminar diffraction pattern is first formed outside the instrument and then focussed on the slit of the spectrograph. The focal length of the lens which forms the pattern and its aperture which is half covered by the retarding plate are entirely at our disposal and may be quite different from those of the dispersing instrument. It is, therefore, possible to obtain what are essentially Talbot's bands with maximum visibility under almost any desired conditions.

Perhaps the most remarkable feature of Talbot's bands is that they involve an alteration of the colour sequence in the spectrum of white light.* Under favourable conditions, a spectrum traversed by the bands appears as an echelon

*N K Sethi, *Philos. Mag.*, 1921, 41, 211.

of colour, presenting as many discrete steps as there are bands instead of the progressive change of hue normally seen in the spectrum. This effect is best exhibited by the bands when the conditions are slightly different from those required for their perfect visibility. Referring again to figure 56, it will be noticed that the line $B_1 B_2 B_3 B_4 B_5$ drawn through the successive maxima of intensity has a slightly greater slope than the line $A_1 A_2 A_3 A_4 A_5$. If, therefore, the dispersion of the spectrograph is about four-fifths of that required for perfect visibility, the intensity maxima in the bands come into coincidence in the spectrum. The dark bands are then not perfectly black, but the proportions of the various wavelengths contributing to the intensity between one minimum and the next remain constant. The result is that the band exhibits a uniform hue, and when we cross from one band to the next, there is a jump in the colour. The effect is most striking when the number of colour steps in the whole spectrum is small, say 3 or 4 or 5. A spectrum of this kind may be obtained by forming the diffraction pattern with a thin plate of mica and resolving it by a prism or grating with relatively small dispersion. With the ordinary arrangements for observing Talbot's bands, the colour jumps may be effectively demonstrated even with as many as 25 or 30 bands in the spectrum, by arranging to move the latter over a slit behind which the eye is placed so as to view the surface of the dispersing prism or grating.

Before leaving this subject, attention may be drawn to the fact that the dispersive power of the retarding plate appears explicitly in the theory of Talbot's and Powell's bands. The significance of this is that, as in all interference experiments with non-homogeneous light, the observed phenomena are determined by the group velocity and not by the wave-velocity of light in the material media. This is very prettily illustrated with Powell's bands when the strongly dispersive mixture of benzene and carbon disulphide is employed to fill the cell in which the retarding glass plate is immersed.* The refractive index of the mixture may be steadily diminished by addition of benzene. Fairly thick plates may be used as the retardations involved depend only on the differences between glass and liquid. The point at which there is equality of refractive index between glass and liquid may be nicely judged by viewing a source of light obliquely through the edge of the plate. It is found that the bands are visible throughout the spectrum at that stage, and continue to be visible until the refractive index is further lowered and the group indices for the glass plate and the liquid mixture are equalised for some particular point in the spectrum. This corresponds to the wavelength at which the bands curve round in figure 55, and as it advances further into the spectrum, the bands on one side of it disappear. If, now, the position of the plate in the cell is reversed, the bands become visible in the part of the spectrum in which they were previously invisible, and *vice versa*.

*N K Sethi, *Phys. Rev.*, 1920, 16, 519.

It may be mentioned that spectra crossed by interferences analogous in principle to Talbot's bands and Powell's bands may be obtained when we have a succession of light beams differing in path by equal amounts (instead of only two) interfering with each other. These may be obtained by using a number of retarding plates in echelon order, or by multiple reflection between parallel surfaces as in a Fabry-Perot etalon or a Lummer-Gehrcke plate. In the latter case, it is necessary to immerse the plate in a dispersive medium.*

Oblique reflection and refraction: The surface of separation between two media differing in their properties is the seat of familiar optical phenomena, viz., reflection, refraction and total reflection. These appear in the electromagnetic theory of light as consequences of the difference in dielectric constant of the two media. By considering the conditions which have to be satisfied at the boundary, which is assumed to be of unlimited area, the laws of reflection and refraction and the intensities of the reflected and refracted beams may be deduced. In the case of total reflection, the theory also leads to the conclusion that there is a superficial disturbance in the second medium. In practice, however, the surface of separation between the two media is of finite extension, and it follows that reflection, refraction and total reflection are necessarily accompanied by diffraction phenomena. We shall now proceed to consider the special features arising in these cases.

The diffraction patterns resulting from the reflection of light at a plane optical surface are easily observed.[†] A prism is set on the table of a spectrometer, and the slit of the collimator is viewed by reflection at one of the surfaces of the prism through the observing telescope. As the incidence of the light on the surface is made more oblique, the image of the slit broadens into diffraction pattern, the extension of which depends on the wavelength of the light employed, the width of the prism face and the angle of incidence. At moderate incidences, the pattern is indistinguishable from that of a rectilinear slit held normally in the path of a parallel beam of light. With increasing obliquity, however, the pattern progressively changes in character and becomes unsymmetrical (see figure 57). The fringes increase in width and at an accelerated rate as we pass from one side of the central fringe to the other. It is evident that on the side of the pattern where the fringes are narrower, there is no specifiable limit to their number, while on the side where they are broader, their number is finite. This limitation of the number of fringes on one side arises from the fact that the pattern does not extend beyond its intersection with the plane of the reflecting surface. Another noteworthy feature is that the corresponding bands on either side of the central band are of very

*N K Sethi, *Phys. Rev.*, 1921, 18, 389.

[†]C V Raman, *Philos. Mag.*, 1906, 12, 494.

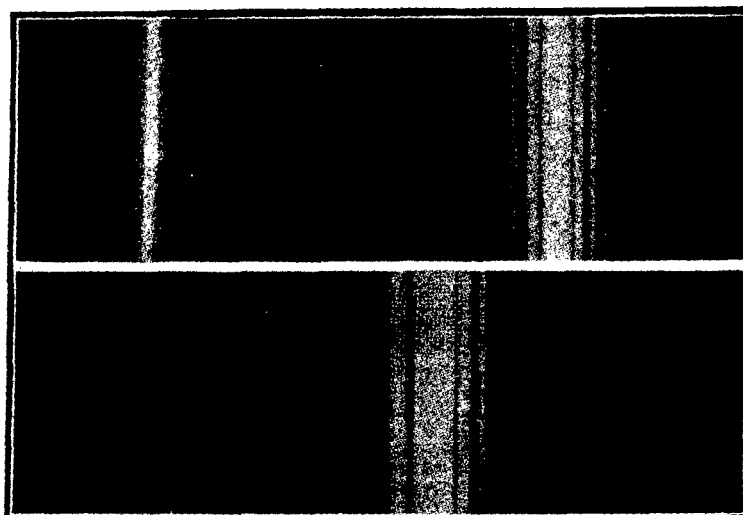


Figure 57. Diffraction patterns of obliquely reflected light.

different intensities. The fringes on the side where they are broader and fewer are much fainter than the corresponding narrow bands on the other side. This difference becomes more conspicuous when the bands compared are respectively nearer and farther from the limit of the pattern. It is also evident that on the side of the pattern remote from this limit, the successive fringes fall off in intensity more slowly than in the normal diffraction pattern of a rectangular aperture.*

Very similar effects are also noticed in oblique refraction at a plane surface. It is well known that an ordinary prismatic spectroscope may be adjusted to give a large dispersion by placing the prism on the table of the instrument in such a position that the light falls at nearly the critical angle of incidence on its second face and emerges in a direction almost parallel to it. There is, however, no gain of resolving power by placing the prism in this position, as the image in the focal plane of the observing telescope is greatly broadened by diffraction. The image is also strongly curved, the deviation being appreciably different for the rays which have passed in slightly different planes through the prism. Owing to the large dispersion produced by the prism, it is necessary to use monochromatic light to observe the diffraction pattern of the obliquely emergent light in the viewing telescope.

Except for the curvature of the fringes and their greater width, the diffraction photographs reproduced in figure 58 for two different angles of emergence are

*C V Raman, *Philos. Mag.*, 1909, 17, 204.

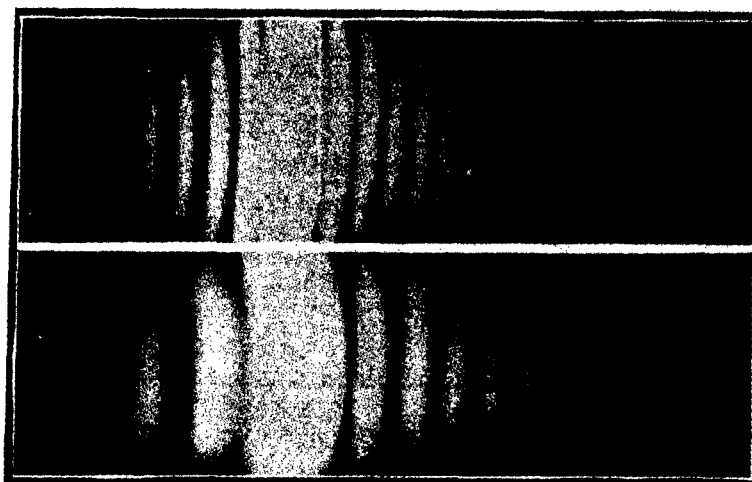


Figure 58. Diffraction patterns of obliquely refracted light.

very similar to the patterns for oblique reflection discussed above and illustrated in figure 57. The fringes show a progressive increase in width from one side of the pattern to the other. Their number on one side is limited by the fact that the plane of the surface of the prism limits the extension of the pattern in that direction. There is also a striking difference in the intensity of the corresponding fringes on either side, the wider fringes being also the fainter. The great number of narrow fringes visible on one side of the pattern indicates that on this side they diminish in intensity more slowly than in the normal diffraction pattern of a rectangular aperture.

With exactly the same arrangements as those used in obtaining the diffraction photographs reproduced in figure 58, if the incidence is increased beyond the critical angle, all the fringes on one side of the pattern and the central fringe move out and disappear, but those on other side persist.* As the angle of incidence is further increased, more fringes move out of the field, but other fringes move into it, with the result that the general appearance of the pattern remains much the same except for the diminished intensity and width of the fringes. Indeed, it is clear that the diffraction phenomena at incidences less and greater than the critical angle form a continuous sequence. The slow diminution in the intensity of the successive fringes observed in figure 59 has evidently the same origin as the corresponding feature in figure 58.

The patterns illustrated in figures 57, 58 and 59 are explicable as interferences of the radiations diffracted by the edges of the surface at which reflection or

*C V Raman, *Philos. Mag.*, 1925, 50, 812.



Figure 59. Diffraction pattern in the second medium in total reflection.

refraction occurs. Alternatively, we may consider them as interferences of the secondary radiations having the elements of area of the reflecting or refracting surface as their origin. Accepting the latter view, we obtain by integration over the surface the expression for the intensity in the pattern, namely,

$$a^2/f\lambda \cdot \cos^2 \psi \cdot \sin^2 \xi / \xi^2$$

where

$$\xi = \pi a(\sin \psi - \sin \psi_0)/\lambda \text{ (for reflection)}$$

$$\xi = \pi a(\sin \psi - \mu \sin \psi_0)/\lambda \text{ (for refraction).}$$

ψ_0 and ψ are the angles of incidence and diffraction respectively. The zeroes of intensity appear at the values of ψ found by making $\xi = \pm \pi, \pm 2\pi, \pm 3\pi$, etc.

A remark is necessary regarding the factor $\cos^2 \psi$ appearing in the foregoing expression for the intensity in the pattern. It results from assuming that the amplitude in the hemispherical secondary waves from the elements of the surface is proportional to the cosine of the angle of diffraction, in other words, that it is greatest at the vortex of a hemisphere and zero at its base. The introduction of this obliquity factor in the law of the secondary wave is found to be necessary for an explanation of the observed distribution of intensity in the patterns. Photometric studies* have confirmed its correctness in the case of reflection† as well as of refraction‡ at individual plane surfaces, as also at a whole series of surface elements lying in a plane and forming a diffraction grating. That the inclusion of the obliquity factor $\cos^2 \psi$ in the expression for the intensity in the pattern is necessary is also indicated by a consideration of the total energy appearing in it. To show this, we may take the case of a perfectly reflecting surface on which light is obliquely incident. The energy received by the surface is that passing through

*C V Raman, *Philos. Mag.*, 1911, 21, 618.

†S K Mitra, *Philos. Mag.*, 1918, 35, 112.

‡B N Chakravarty, *Proc. R. Soc. London*, 1921, A99, 503.

an area $a \cos \psi_0$ of the incident beam, and the same should appear in the diffraction pattern. The energy actually appearing in the latter according to our formula is

$$\int \frac{a^2}{f\lambda} \cdot \cos^2 \psi \cdot \frac{\sin^2 \xi}{\xi^2} \cdot f \cdot d\psi,$$

and this may be written in the form

$$\int \frac{a}{\pi} \cdot \cos \psi_0 \cdot \frac{\cos \psi}{\cos \psi_0} \cdot \frac{\sin^2 \xi}{\xi^2} \cdot d\xi.$$

This permits of being equated to $a \cos \psi_0$. For, the integral of $\sin^2 \xi / \xi^2$ with respect to ξ when a sufficient number of fringes is present on both sides of the pattern is π ; in such an integration, we may without sensible error write ψ equal to ψ_0 , its value for the central fringe which contains the largest part of the total energy. On the other hand, when some of the fringes in the part of the pattern where $\psi > \psi_0$ have disappeared, the loss of their contribution to the integral would be compensated for by the increased intensity of fringes for which $\psi < \psi_0$.

It is worthy of remark that the diffraction of light obliquely emergent from a plane surface plays an essential role in the operation of the well known and valuable instrument known as the Lummer–Gehrcke plate. It is not unusual to find this described as an interferometer. The theory of the instrument as actually employed is, however, far from being that of a simple interference plate. In practice (see figure 60), the light is admitted into it through a reflecting prism cemented or optically attached to one end, and the reflection at the external surface of the plate is thus avoided. This makes the plate a “direct-vision” instrument and results in a large gain of illumination. As a result of this arrangement, also, we have *exactly* similar patterns on both sides of the plate, and the complementary character of the results as observed by transmitted and reflected light is no longer in evidence. In other words, *the Lummer plate functions as a diffraction grating and not as a simple interference plate*. Corresponding to a definite direction of incidence within the plate, the direction of emergence of the light may coincide with any one of several orders of interference. That this should happen is not surprising, as the individual beams emerging from the plate very obliquely are necessarily of limited aperture and are, therefore, immensely widened by diffraction. Though, in practice, an extended source of light is

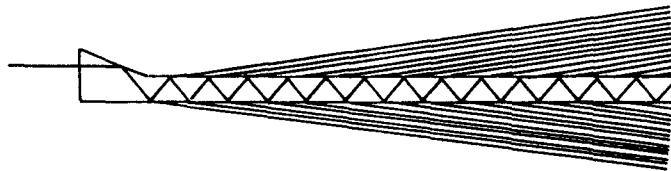


Figure 60. Diagram of the Lummer–Gehrcke plate.

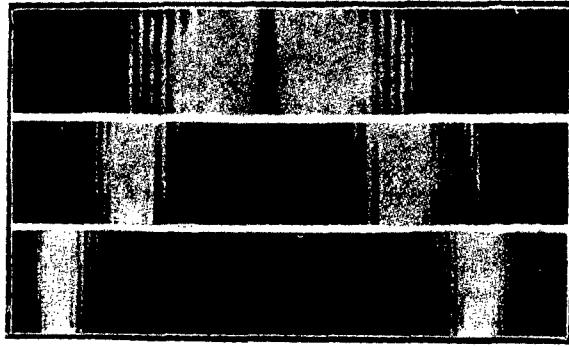


Figure 61. Lummer patterns at different incidences.

employed, this is not essential and the pattern may be observed even with a narrow slit, and indeed even when the light is incident within the plate at more than the critical angle. This is shown by the photographs reproduced in figure 61 which were obtained with the full aperture of the plate and with various incidences, using the 4358 A.U. radiations of the mercury lamp.

Figure 61 shows that the position of the interferences remain unaffected, though the distribution of intensity amongst them alters, when the angle of incidence of the light is varied. This circumstance which enables an extended source of light to be used for observing the interferences follows as a consequence of the Fermat principle of stationary path. If θ and ϕ are the glancing angles of incidence and emergence of the light beams for a given order of interference, λ and μ being respectively the wavelength of the light and the refractive index of the plate, it is readily shown that $d\phi/d\lambda$ has the same value whether we regard the arrangement as an interference plate or as a diffraction grating. In the former case, we vary both θ and ϕ and maintain the geometric relation $\cos \phi = \mu \cos \theta$ between them. In the latter case, we keep θ constant and vary ϕ maintaining the path-difference between the successive diffracted beams as a constant multiple of the wavelength. In either case, we obtain the same result, namely,

$$\sin \phi \frac{d\phi}{d\lambda} = \frac{1}{\lambda \cos \theta} \left(\mu \sin^2 \theta - \lambda \frac{d\mu}{d\lambda} \right).$$

The aggregate aperture of the emerging pencils is $l \sin \phi$, where l is the length of the plate; the ratio of this to the wavelength determines the angular width of the diffraction maxima and, therefore, also the resolving power of the instrument. The latter may be evaluated by writing $d\phi = \lambda/l \sin \phi$ in the preceding formula, and we thus obtain

$$\frac{\lambda}{d\lambda} = \frac{l}{\lambda \cos \theta} \left(\mu \sin^2 \theta - \lambda \frac{d\mu}{d\lambda} \right).$$

The phenomena of total reflection: Total reflection was first explained on wave-principles by Huygens. Assuming that secondary wavelets issue from the surface into both media, he showed that when the incidence is beyond the critical angle, no common envelope can be drawn to the wavelets in the second medium and no resultant wave can, therefore, emerge into it. Supplementing this argument by the principle of interference, it can be rigorously proved that there should be a superficial disturbance in the second medium. It will be useful first to show this in an elementary way by the familiar method of the Fresnel zones. To mark out the form of the zones on the surface, we consider some particular point of observation in the second medium and drop a perpendicular from it on the surface. Around the foot of this perpendicular as centre, circles are drawn of which the distances from the point of observation increase successively by units of half a wavelength. Parallel and equidistant straight lines are similarly drawn perpendicular to the plane of incidence and indicating the points on the surface at which the phase of the incident plane waves differs by half a period. Both the circles and straight lines are serially numbered, and by adding these numbers at the points of intersection, the points of constant total path may be found and curves drawn through these to represent the Fresnel zones on the surface for the particular point of observation. The form of the zones thus derived and the changes in their configuration with the angle of incidence and the position of the point of observation enable us to obtain a general and comprehensive view of the case.* The zones are closed curves only when the angle of incidence is less than the critical angle; at and beyond the critical incidence, they open out and assume approximately hyperbolic forms. It is evident that there are no poles or points of stationary phase on the surface at such incidences, and the disturbance in the second medium is, therefore, a residual or diffraction effect.

Considering the disturbance at some point fairly close to the surface, it is evident that the contribution to this from distant parts of the surface is insignificant. For, the obliquity factor being the cosine of the angle which the diffracted ray makes with the normal to the surface, the effect of such parts of the surface becomes vanishingly small. On the other hand, the parts of the surface near the points of observation have the maximum value of the obliquity factor, namely, unity. In this region, remarkable changes in the form of the Fresnel zones are observed if the point of observation is at or near the surface. Figure 62 shows the form of the zones for a case in which the incidence is at 60° , the critical angle being 45° , while the point of observation is on the surface itself. Figure 63 shows the zones for the same case when the point of observation is at a distance of 4λ from the surface. A sudden discontinuity in the width of the Fresnel zones to the

*C V Raman, *Proc. Indian Assoc. Cultiv. Sci.*, 1926, 9, 271 and 330, (The second reference contains some remarks on the sharpness of the boundary of critical reflection as affected by diffraction when the aperture is limited.)

right and left of the origin will be noticed in figure 62. Accordingly, there must be a large resultant effect at this point. In figure 63, the discontinuity has disappeared, there being now a steady increase in the width of the zones as we pass from one side of the origin to the other. Accordingly, the effects of the Fresnel zones should cancel each other out by interference. The configuration of the Fresnel zones thus clearly indicates that there is a strong superficial disturbance

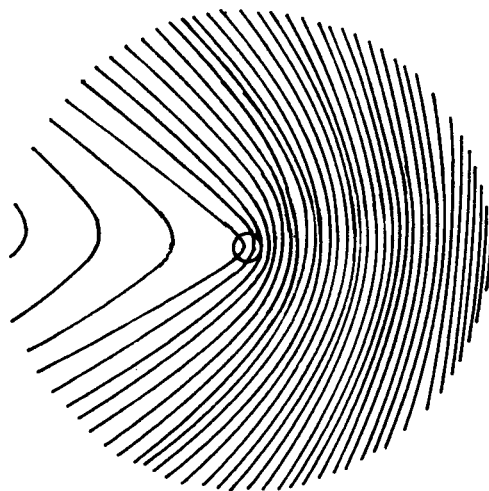


Figure 62. Form of Fresnel zones on surface. Incidence at 60° (critical angle 45°); point of observation on surface.

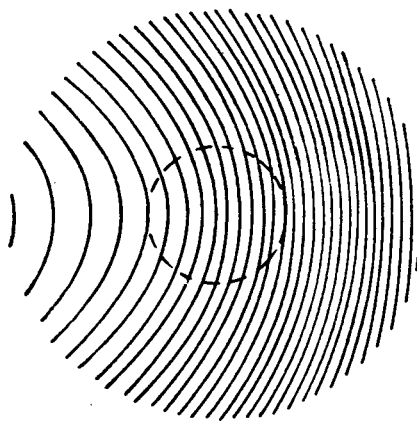


Figure 63. Form of Fresnel zones; incidence at 60° (critical angle 45°); point of observation 4λ from surface.

in the second medium, and that this diminishes rapidly as we move away from the surface. The further we are from the critical incidence, the more quickly does this diminution occur.

When the point of observation is sufficiently removed from the surface, the contribution from the neighbouring parts of the surface becomes entirely negligible. On the other hand, the effects arising at the margin of the illuminated area of the surface then come into prominence. The magnitude of these effects depends on two factors, namely, the width of the uncompensated zones at the edges, and the obliquity factor. These factors work in opposite directions, since the width of the zones would be greatest when the direction of observation is parallel to the surface, while in this direction the obliquity factor actually vanishes. The most suitable way of observing the edge effects is to view them obliquely from a point entirely outside the surface and in a direction nearly parallel to it. Both the rear and front edges then appear as fine luminous lines and are seen to be of equal intensity. The interference of the edge radiations gives rise to a diffraction pattern which can be recorded photographically with sufficiently long exposures* (see figure 59).

Returning to the effects observed at a point P near the surface, we may derive an expression for the superficial wave in the second medium. The perpendicular drawn from P to the surface is taken as z -axis, its foot as the origin, and the plane of incidence of the light as the XZ plane. The light vector in the first medium along the surface may be assumed to be of the form

$$A\sigma_0 \cdot \cos(Q_0 - 2\pi x \sin \psi_0/\lambda), \text{ or simply } A\sigma_0 \cdot \cos Q$$

for brevity, σ_0 being an undetermined constant. The surface is divided up into elements of area $\rho d\rho d\phi$ in polar co-ordinates, r the distance of the element from P being $(z^2 + \rho^2)^{1/2}$. The effect of the secondary wave from such an element at P is

$$A\sigma_0 \cdot \frac{\rho d\rho d\phi}{\lambda r} \cdot \cos(Q - 2\pi\mu \cdot \rho \sin \psi_0 \cos \phi/\lambda - 2\pi r/\lambda).$$

The obliquity factor is taken as unity, since the effect at P is mainly due to elements on the surface near the origin. Integrating with respect to ϕ between the limits 0 and 2π , we obtain the resultant effect at P as

$$A\sigma_0(C \cos Q + S \sin Q)$$

*C V Raman, *Philos. Mag.*, 1925, 50, 812.

where C and S respectively stand for

$$C = \frac{2\pi}{\lambda} \int_0^\infty J_0\left(\frac{2\pi\mu\rho \sin \psi_0}{\lambda}\right) \cos \frac{2\pi r \rho d\rho}{\lambda r}$$

$$S = \frac{2\pi}{\lambda} \int_0^\infty J_0\left(\frac{2\pi\mu\rho \sin \psi_0}{\lambda}\right) \sin \frac{2\pi r \rho d\rho}{\lambda r}.$$

These are well known integrals.* When $\mu \sin \phi_0 > 1$, S vanishes and the effect at P reduces† to

$$A\sigma_0(\mu^2 \sin^2 \psi_0 - 1)^{-1/2} \cos Q \cdot \exp(-2\pi z \sqrt{\mu^2 \sin^2 \psi_0 - 1/\lambda})$$

$$= A\sigma \cos Q \cdot \exp(-2\pi z \sqrt{\mu^2 \sin^2 \psi_0 - 1/\lambda})$$

thus appearing as a superficial wave $A\sigma \cos Q$ at the surface and travelling along the x -axis, the amplitude of which decreases exponentially with the distance z from the surface. The disturbance at the surface in the first medium is due jointly to the incident and totally reflected waves. If these are individually

$$A \cos(Q - \delta/2) \quad \text{and} \quad A \cos(Q + \delta/2),$$

their resultant is $2A \cos \delta/2 \cos Q$. The continuity of the disturbance at the surface parallel to the y -axis requires that $\sigma = 2 \cos \delta/2$, thus showing that the amplitude σ of the superficial wave and the phase change δ in total reflection are closely connected with each other. To evaluate σ and δ , we require a second relation. This is obtained by considering the continuity of the disturbance parallel to the x -axis on the two sides of the boundary. If the electric vector in the incident waves is parallel to the y -axis, then the magnetic vector H_x , i.e., $\partial E_y/\partial z$ must be the same on the two sides of the boundary. If, similarly, the magnetic vector in the incident waves is parallel to the y -axis, then the electric force E_x must be the same on the two sides; in other words

$$\left(\frac{\partial H_y}{\partial z}\right)_1 = \mu^2 \left(\frac{\partial H_y}{\partial z}\right)_2.$$

Applying these conditions, the values of σ and δ in these two cases are respectively

*Bateman's *Electrical and Optical Wave-Motion*, p. 72; and Watson's *Treatise on Bessel Functions*, 1922, p. 416.

†C V Raman, *Trans. Opt. Soc. Am.*, 1927, 28, 149.

found to be

$$\sigma_s^2 = \frac{4\mu^2 \cos^2 \psi_0}{\mu^2 - 1}, \quad \tan \frac{1}{2}\delta_s = \frac{\sqrt{\mu^2 \sin^2 \psi_0 - 1}}{\mu \cos \psi_0}$$

$$\sigma_p^2 = \frac{4 \cos^2 \psi_0}{(1 - \mu^2) + (\mu^4 - 1) \sin^2 \psi_0}, \quad \tan \frac{1}{2}\delta_p = \frac{\sqrt{\mu^4 \sin^2 \psi_0 - \mu^2}}{\cos \psi_0}.$$

It is readily verified that at the critical incidence, $\delta_s = \delta_p = 0$ and $\sigma_s = \sigma_p = 2$. In other words, the amplitude of the superficial disturbance which is then a maximum is the arithmetic sum of the amplitudes in the incident and reflected waves. At grazing incidence, $\delta_s = \delta_p = \pi$, and $\sigma_s = \sigma_p = 0$. In other words, the surface is a nodal plane and the superficial wave vanishes. At intermediate incidences, δ_p is greater than δ_s , and this results, when the incident light is plane polarised in an azimuth inclined to the plane of incidence, in the reflected light being elliptically polarised.

The existence of a superficial wave in the second medium may be demonstrated in several ways. A direct method which has the advantage of enabling us to determine the distribution of intensity in depth as well as direction of energy flow and the state of polarisation, is to use the well known property possessed by a sharp metallic edge of diffracting a stream of radiation falling upon it.* A fresh safety razor-blade is held normal to the surface of a totally reflecting prism and with its edge exactly parallel to it. A fine slow-motion of the kind provided in interferometers enables the blade to be moved forward or backward by fractions of a wavelength. The razor edge is viewed through a microscope focussed on it. If the axis of the microscope is in the plane of incidence of the light, and the razor-blade is perpendicular to it, the edge when slowly advanced to within a very small distance of the surface, becomes visible as a fine luminous line. The intensity is greatest when the axis of the microscope is as nearly as possible parallel to the surface. The distance from the surface within which the luminosity of the edge is perceptible is a measure of the thickness of the superficial disturbance. It is known that a diffracting edge is only luminous when seen along the surface of a cone having the edge as axis and the ray incident on it as a generating line. Hence the observations indicate that the direction of energy-flow in the superficial disturbance is in the plane of incidence and parallel to the surface. When the incidence is just at the critical angle, the intensity of the superficial wave is found to be a maximum and comparable with that of the incident and reflected waves. As the incidence is increased, the intensity falls off very quickly. The decrease of intensity with increasing distance from the surface is also rapid. When the incidence is not much greater than the critical angle, say about 50° for glass, the

*C V Raman, *Trans. Opt. Soc. Am.*, 1927, 28, 149.

luminosity is perceptible when the edge is within a wavelength or so from the surface. For larger angles of incidence, the decrease is much more rapid, and the luminosity is perceptible only when the edge is practically in actual contact with the prism. When the incident light is polarised, the edge radiation is found to be partially polarised, the stronger component of the electric vector being perpendicular to the edge. This is in accord with the theoretical expectations.

Diffraction of light by curved surfaces: A convex rounded edge on which light is incident reflects the light falling upon it, and the superposition of this on the exterior diffraction increases its apparent intensity, and makes it perceptible over larger angles. On the other hand, the light bending into the region of shadow is diminished in intensity by reason of the curvature of the edge and its visibility is restricted to smaller angles. This effect may be observed with edges having a curvature which may lie within wide limits and is expressible in microns or centimetres or even metres. The angles involved and the magnitude of the effects would, however, naturally depend on the radius of curvature. A typical experiment demonstrating the effect under consideration is the comparison of the intensities of the bright spots seen at the centre of a shadow of a circular disk and of a spherical ball of the same radius.* To make the comparison significant, the disk should have a sharp edge, while the ball should be an accurately made sphere with a highly polished surface. The ball and disk may be set side by side and held in the path of a beam of light from a point-source of light. The spots at the centre of their respective shadows may then be directly viewed and their intensities photometrically compared.

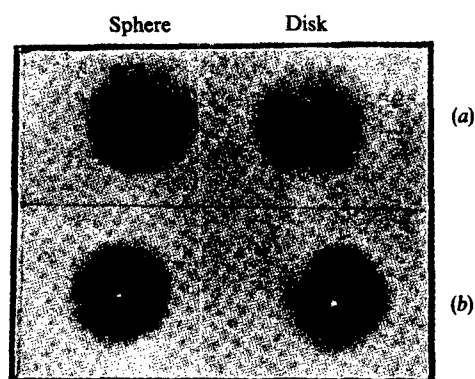


Figure 64. Diffraction by sphere and disk of equal diameter (1.5 cm) and at (a) 40 cm, and (b) 120 cm distances from them.

*C V Raman and K S Krishnan, *Proc. Phys. Soc.*, 1926, 38, 350.

A great difference is noticed in the brightness of the two spots. This difference increases as we approach the objects (figure 64); the intensity of the spot for the sphere falls off more quickly than for the disk, becoming a very small fraction of it. At a distance of 120 centimetres, the difference of the intensities is still perceptible, while at greater distances, the two spots tend gradually to approach equality of brightness.

The diffraction of light by convex cylindrical edges similarly shows interesting features. If the radius of curvature of the edge is of the order of a few centimetres, the phenomena in the vicinity of the edge may be conveniently studied with a distant slit parallel to the cylinder as the source of light and a microscope for viewing the fringes.* The effects are, however, more striking when a strip of mirror glass, 3 centimetres wide and 75 centimetres long, is bent into a cylindrical shape of large radius of curvature. The diffraction fringes produced by it can be seen directly on a screen or viewed with an ordinary magnifier.† The general nature of the case will be evident when we consider the rays of light which pass by the cylinder without meeting its surface and those which fall on it and are reflected. These form the two branches of a cusped wave-front which is fully developed at the edge of the cylinder grazed by the incident rays. The two branches interfere, giving fringes parallel to the edge, their number and visibility being greatest when the plane of observation is that of the edge itself. As we move away from this plane, the intensity of the reflected rays diminishes more quickly on account of their divergence. The visibility of the fringes, therefore, falls off until, finally, they are scarcely distinguishable from the usual type of diffraction bands along the boundary of the shadow of a straight edge. The law of the spacing of these fringes may be readily deduced. If a is the radius of the cylinder, and d the distance of the plane of observation from its edge, the distance x of the maxima and minima of the illumination from the edge of the geometric shadow may be found by eliminating ϵ from the two equations

$$x = 2\epsilon d + 3\epsilon^2 a/2 \quad \text{and} \quad n\lambda = 4\epsilon^2 d + 4\epsilon^3 a.$$

When d is much larger than a , we have $x = \sqrt{n\lambda d}$, and the positions of the fringes differ only slightly from those in the diffraction pattern due to a straight edge for which we have $x = \sqrt{(n - \frac{1}{4})\lambda d}$. Indeed except in the vicinity of the cylinder, the spacing of the fringes is scarcely different from that due to a sharp straight edge, the principal difference being in the greater number and the visibility of the fringes. Phenomena of the same nature are also observed in the exterior diffraction by

*N Basu, *Philos. Mag.*, 1918, 35, 79.

†T K Chinmayanandam, *Philos. Mag.*, 1919, 37, 9. The same procedure may be used for observing the optical analogue of the whispering gallery effect with a concave surface.

reflecting obstacles of other forms having a convex surface, e.g., cones, spheres or ellipsoids.*

The rapidly diminishing intensity of the light entering the region of shadow and its restriction to smaller angles with increased radius of curvature of the surface are facts of observation which require explanation. Some light is thrown on the matter by a consideration of the facts regarding the diffraction of light by metallic screens dealt with earlier in this lecture. An examination of the formulae shows that the nature of the results to be expected is greatly influenced by the angle of incidence of the light on the surface of the screen.[†] When the incidence is sufficiently oblique, both components of the electric vector in the diffracted rays parallel to the surface of the screen become of equal intensity, and are quite small. This indication of theory is in accord with observation,[‡] and may be expected to be true for all reflecting surfaces whether metallic or not. In our present problem, we are concerned with the diffraction of light which is incident very obliquely or actually grazes the surface of the obstacle. Hence, unless the radius of curvature of the obstacle is very small, the polarisation effects would be negligible and both components of the diffracted light would be weak along its surface. The greater the radius of curvature, the longer the arc of the surface which the diffracted ray has to graze before it can emerge at any desired angle. Hence, the attenuation of

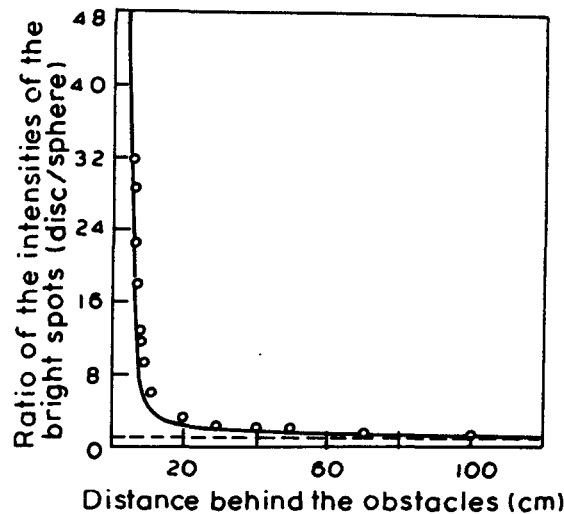


Figure 65. Comparison of theoretical attenuation factor and experimental data.

*A B Datta, *Bull. Calcutta Math. Soc.*, 1922.

†C V Raman and K S Krishnan, *Proc. R. Soc. London*, 1927, 116, 254.

‡S K Mitra, *Philos. Mag.*, 1919, 37, 50.

the diffracted light must increase rapidly with the radius of curvature. The problem here considered is evidently analogous to that of the bending of electric waves around the surface of the earth. The attenuation factor for the amplitude in this case* is $\exp(-0.70(2\pi a/\lambda)^{1/3}\theta)$, where a is the radius of the earth, λ the wavelength and θ the angle which the waves have to creep round. The formula indicates a rapid fall in the intensity of the radiation as it bends round, if the radius of curvature of the edge is large compared with the wavelength, and this is in accord with actual experience in the optical problem.

The measurements† made of the relative intensity of the bright spots in the shadow of a sphere and a disk of equal diameter at different distances along the axis enable a quantitative test to be made of the attenuation formula quoted above. The arc over which the diffracted waves have to creep may be taken as zero for the sharp-edged disk. For the sphere, it is the arc on the surface between the circles of contact with the tangent cones drawn to it respectively from the point-source of light and from the point of observation. Figure 65 shows the theoretical attenuation curve for this case, the experimental data being indicated by dots. The general agreement leaves little doubt that the explanation of the facts which has been put forward is on the right lines.

* Riemann-Weber, *Differential-Gleichungen Phys.*, 1927, 2, 594.

† C V Raman and K S Krishnan, *Proc. Phys. Soc.*, 1926, 38, 350.